doi:10.1093/plphys/kiaa033 PLANT PHYSIOLOGY 2021: 185: 331–351

Plant Physiology

Research Article

Plant apocarotenoid metabolism utilizes defense mechanisms against reactive carbonyl species and xenobiotics

Julian Koschmieder [1], Florian Wüst [1], Patrick Schaub [1], Daniel Álvarez [1,†], Danika Trautmann,[1,2] Markus Krischke [3], Camille Rustenholz [2], Jun'ichi Mano [4,5], Martin J. Mueller [2], Dorothea Bartels [6], Philippe Hugueney [3], Peter Beyer [1] and Ralf Welsch [1,*,‡]

1 Faculty of Biology II, University of Freiburg, 79104 Freiburg, Germany
2 Université de Strasbourg, INRAE, SVQV UMR-A 1131, F-68000 Colmar, France
3 Julius-Maximilians-University Würzburg, Julius-von-Sachs-Institute for Biosciences, Julius-von-Sachs-Platz 2, 97082 Würzburg, Germany
4 Science Research Center, Organization for Research Initiatives, Yamaguchi University, Yoshida 1677-1, Yamaguchi 753-8515, Japan
5 Graduate School of Sciences and Technology for Innovation, Yamaguchi University, Yoshida 1677-1, Yamaguchi 753-8515, Japan
6 Institute of Molecular Physiology and Biotechnology of Plants, University of Bonn, Kirschallee 1, 53115 Bonn, Germany

*Author for communication: ralf.welsch@biologie.uni-freiburg.de
†Present address: The International Center for Tropical Agriculture (CIAT), Km 17, Recta Cali-Palmira, Colombia.
‡Senior author.

R.W., J.K., and P.B. designed the research; R.W., J.K., F.W., P.S. performed the research; D.A., D.T., and C.R. performed RNA isolation and RNASeq raw data processing, respectively; M.K. performed HOTE analysis; P.H., M.M., D.B., and J.M. contributed analytical tools and cDNAs; R.W. and J.K. wrote the article.

The author responsible for distribution of materials integral to the findings presented in this article in accordance with the policy described in the Instructions for Authors (https://academic.oup.com/plphys) is: Ralf Welsch (ralf.welsch@biologie.uni-freiburg.de).

Abstract

Carotenoid levels in plant tissues depend on the relative rates of synthesis and degradation of the molecules in the pathway. While plant carotenoid biosynthesis has been extensively characterized, research on carotenoid degradation and catabolism into apocarotenoids is a relatively novel field. To identify apocarotenoid metabolic processes, we characterized the transcriptome of transgenic Arabidopsis (*Arabidopsis thaliana*) roots accumulating high levels of β-carotene and, consequently, β-apocarotenoids. Transcriptome analysis revealed feedback regulation on carotenogenic gene transcripts suitable for reducing β-carotene levels, suggesting involvement of specific apocarotenoid signaling molecules originating directly from β-carotene degradation or after secondary enzymatic derivatizations. Enzymes implicated in apocarotenoid modification reactions overlapped with detoxification enzymes of xenobiotics and reactive carbonyl species (RCS), while metabolite analysis excluded lipid stress response, a potential secondary effect of carotenoid accumulation. In agreement with structural similarities between RCS and β-apocarotenoids, RCS detoxification enzymes also converted apocarotenoids derived from β-carotene and from xanthophylls into apocarotenols and apocarotenoic acids in vitro. Moreover, glycosylation and glutathionylation-related processes and translocators were induced. In view of similarities to mechanisms found in crocin biosynthesis and cellular deposition in saffron (*Crocus sativus*), our data suggest apocarotenoid metabolization, derivatization and compartmentalization as key processes in (apo)carotenoid metabolism in plants.

Received August 18, 2020. Accepted November 8, 2020. Advance access publication December 1, 2020

Introduction

Carotenoids are isoprenoids exerting an immense repertoire of functions in almost all aspects of plant physiology and development. They are essential photosynthetic pigments, serve as substrates for phytohormone biosynthesis, and provide coloration for fruits and flowers (Yuan et al., 2015; Baranski and Cazzonelli, 2016). Over the past decades, knowledge on the carotenoid biosynthesis pathway in plants has become very well-established and extensively reviewed (Cazzonelli and Pogson, 2010; Wurtzel, 2019), whereas the understanding of carotenoid catabolism has started to improve significantly in recent years.

Enzymatic carotenoid cleavage by specific carotenoid cleavage dioxygenases (CCDs) and nine-*cis*-epoxy-carotenoid dioxygenases (NCEDs) in plants can result in highly specific cleavage into apocarotenoids, exerting explicit functions either directly or after modification (Ahrazem et al., 2016; Hou et al., 2016). This applies to strigolactone (SL) biosynthesis, involving CCD7/more axillary branching 3 (MAX3) and CCD8/MAX4 (Alder et al., 2012; Wang and Bouwmeester, 2018), and to abscisic acid (ABA) biosynthesis, involving several NCEDs (Tan et al., 2003). At the same time, CCD1 and CCD4 initiate catabolic routes, initially yielding a plenitude of apocarotenoids of different chain lengths by nonspecific cleavage at different cleavage sites (Simkin et al., 2004; Rubio et al., 2008, Ilg et al., 2009; Bruno et al., 2015). Additionally, the same diversity of apocarotenoids is also formed by nonenzymatic carotenoid degradation, resulting from the antioxidant properties of carotenoids. The two processes occur simultaneously and apocarotenoids undergo further derivatization (Walter and Strack, 2011; Lätari et al., 2015; Schaub et al., 2018).

The dynamic equilibrium between degradation and biosynthesis in plant tissues determines the steady-state carotenoid levels (Simkin et al., 2003; Lätari et al., 2015). Accordingly, high carotenoid levels in plant tissues are the result of high biosynthetic activity and/or by attenuated degradation, the latter often being achieved by carotenoid sequestration. Interestingly, if carotenoid-sequestrating structures are absent and carotenoid biosynthesis rates are low—for instance during storage of ripe seeds, vegetables, and fruits—β-carotene (provitamin A) contents steadily decrease at varying rates (Beyer et al., 2002; Schaub et al., 2017, 2018).

Nonenzymatic degradation of carotenoids is due to the highly unsaturated hydrocarbon backbone being susceptible to oxidation, generating epoxy- and peroxide derivatives as well as polymeric aggregates. Upon oxidation, carotenoids decompose into apocarotenoids and finally form a plethora of products partially identical to those formed enzymatically (Britton, 1995; Burton et al., 2014, 2016; Schaub et al., 2017, 2018). Several lines of evidence suggest that nonenzymatic oxidation rates surpass those for enzymatic cleavage, i.e. degradation rather than enzyme-driven catabolism appears to be the main determinant of carotenoid levels, besides carotenoid biosynthesis. In chloroplasts, photooxidation is the predominant carotenoid degrading process and produces apocarotenoids involved in light stress signaling (Simkin et al., 2003; Beisel et al., 2010; Ramel et al., 2012b; Lätari et al., 2015). Moreover, carotenoid levels in *ccd1* and *ccd4* mutants are not notably affected (Gonzalez-Jorge et al., 2013; Lätari et al., 2015). In most tissues, the carotenoid pathway flux is surprisingly high in relation to the amounts of carotenoids accumulating. For instance, the synthesis rates can be visualized by application of the inhibitor norflurazone, resulting in an unexpectedly high accumulation of oxidation-resistant phytoene (Simkin et al., 2003; Lätari et al., 2015; Koschmieder and Welsch, 2020). However, levels of apocarotenoids are by far not quantitatively equivalent to carotenoid losses (Schaub et al., 2017, 2018). Therefore, it can be hypothesized that these primary cleavage products might be further metabolized by secondary cleavage reactions targeting the remaining double bonds (Figure 1), by formation of conjugates and of polymeric aggregates (Burton et al., 2014; Lätari et al., 2015) as well as by so far unknown reactions.

Most apocarotenoids contain highly reactive α,β-unsaturated carbonyl moieties (see Figure 1), representing reactive electrophiles (RES) or reactive carbonyl species (RCS). The toxicity of α,β-unsaturated carbonyls like RCS originates from the reactivity of the α,β-unsaturated C-C double bond with its high electrophilicity and capability of forming Michael adducts with thiol and amino groups as well as from the ability of the aldehyde group to form Schiff bases (Yamauchi et al., 2011). These reactive carbonyl functions induce detoxification responses mediating their metabolization, thereby preventing the accumulation of cytotoxic cellular components (Farmer and Davoine, 2007). In the last decade, the understanding of RCS detoxification in plants has substantially progressed and similarities with the more extensively studied RCS detoxification in yeast and animals have been unraveled (for review, see Mano, 2012; Mano et al., 2019a). Upon corresponding stimuli, RCS are generated downstream of the formation of reactive oxygen species and function as signaling compounds, which induce a set of RCS detoxifying enzymes. However, the occurrence of equivalent detoxification reactions with apocarotenoids has not been investigated so far.

The carotenoid biosynthesis pathways starts from isopentenyl diphosphate, produced via the plastid-specific methylerythritol phosphate pathway (MEP; Yuan et al., 2015). The enzyme phytoene synthase (PSY) catalyzes the formation of phytoene from two molecules of geranylgeranyl diphosphate (GGPP). Upon desaturation by phytoene desaturase (PDS) and ζ-carotene desaturase (ZDS), isomerization by ζ-carotene isomerase (Z-ISO) and carotene *cis–trans* isomerase (CrtISO) and cyclization by lycopene α- and β-cyclase, α- and β-carotene are formed, respectively (Cazzonelli and Pogson, 2010; Wurtzel, 2019). Hydroxylations by four enzymes produce various xanthophylls with important photoprotective functions (Kim et al., 2009).

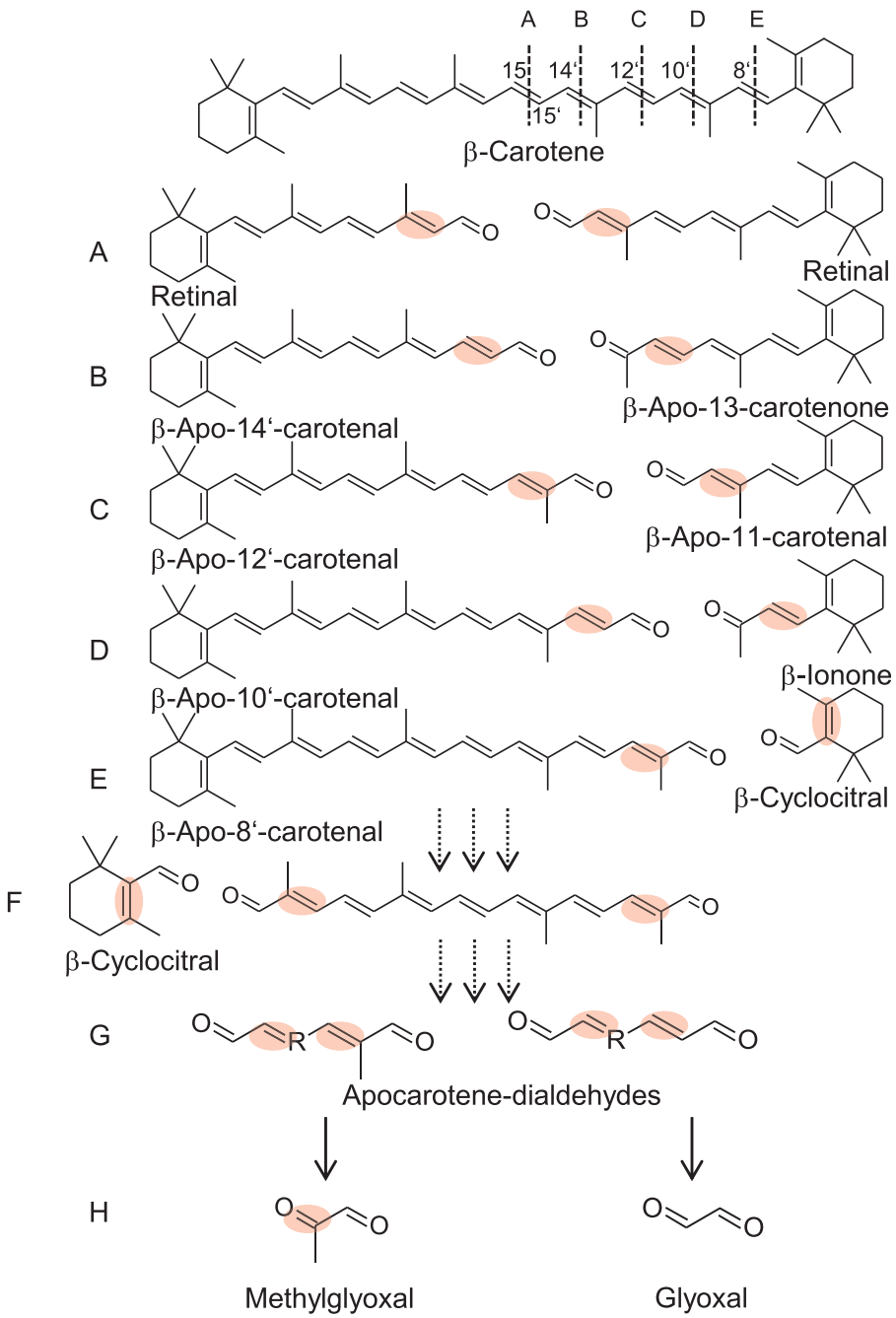

Figure 1 β-Carotene oxidation products. β-Carotene oxidation primarily yields β-apocarotenoids of various chain lengths. Numbers indicate the reacting double bond position; the corresponding cleavage product pairs are depicted below β-carotene from (**A**) to (**E**). Secondary oxidation results in the release of the β-ionone ring moiety, e.g. as β-cyclocitral, and linear apocarotene-dialdehydes, shown in (**F**) and (**G**). (**H**) Methylglyoxal and glyoxal represent end products after continued oxidation of carotene dialdehydes. Highly reactive α,β-unsaturated double bonds are marked with a red dot.

In the present work, we investigated β-apocarotenoid metabolism by analyzing the transcriptome of Arabidopsis (*Arabidopsis thaliana*) engineered to overaccumulate β-carotene and, consequently, β-apocarotenoids. This was achieved by the overexpression of *PSY*, often rate-limiting in carotenogenesis and sufficient to raise total carotenoids (Welsch et al., 2008, 2017; Farré et al., 2010, Álvarez et al., 2016). We used roots as a model system to identify metabolic processes of β-carotene, using wild-type (WT) roots with their low background of carotenoid metabolism as the comparator. The plant's response to induced accumulation of β-apocarotenoids allowed unraveling a set of enzymes, which had so far been associated with the detoxification of RES and RCS. Furthermore, we describe a specific feedback regulation that appears to counteract β-carotene accumulation upon *PSY* overexpression. This might be mediated by β-apocarotenoids

or their derivatives, providing insight into mechanisms associated with the regulation of carotenoid homeostasis in plants.

Results

Metabolite and transcriptome analysis of β-carotene accumulating Arabidopsis roots

Increased carotenoid pathway flux results in β-carotene crystallization in Arabidopsis callus and roots, but simultaneously primary β-carotene oxidation products—β-apocarotenoids—increase in abundance (Maass et al., 2009; Schaub et al., 2018). We hypothesized that efficient degradation mechanisms would be upregulated in response to enhanced β-apocarotenoid levels. Therefore, *PSY*-overexpressing Arabidopsis roots were used to identify and characterize β-apocarotenoid-specific metabolic processes by combining metabolic and transcriptomic analyses.

We determined the profile of carotenoids and β-carotene-derived apocarotenoids in roots from hydroponically grown WT and *PSY*-overexpressing Arabidopsis plants (*At12* and *At22*) by liquid chromatography–mass spectrometry (LC–MS). As often observed upon *PSY* overexpression in various taxa, xanthophyll and α-carotene amounts increased moderately, while especially β-carotene isomer amounts increased very strongly, from 2-μg g^{-1} DM (dry mass) in WT roots to 162- or 278-μg g^{-1} DM for the all-*trans*-isomer in *At22* and *At12*, respectively (Figure 2A). Pathway intermediates like phytoene, phytofluene, ζ- and γ-carotene accumulated exclusively in *PSY*-overexpressing lines, being undetectable in WT roots. Total carotenoid content of *PSY*-overexpressing roots increased 37- to 61-fold or up to 370.3 ± 14.3 and 613.2 ± 31.2 μg g^{-1} DM for *At22* and *At12*, respectively, while only 10.0 ± 0.6 μg g^{-1} DM accumulated in WT roots. The accumulated β-carotene isomers accounted for 58% of carotenoid increase in *At22* and *At12* (and phytoene for 25%).

Similar to our previous observation made with carotenoid-accumulating calli, β-apocarotenoid amounts strongly increased (Figure 2B). For instance, retinal and β-apo-13-carotenone amounts increased 2-fold, while β-apo-8-carotenal, β-apo-10-carotenal, β-apo-12-carotenal, β-apo-14-carotenal, and β-apo-11-carotenal increased up to 20-fold compared to WT roots. We also determined the relative abundance of apocarotene dialdehydes, which can originate from almost all fully desaturated carotenoids by double cleavage at both ends and from apocarotenoid cleavage at the uncleaved end (Benevides et al., 2011). Short-chain apocarotene dialdehydes (C_5-, C_8-, and C_{10}-dialdehydes) accumulated up to 10-fold compared to the control (Figure 2C), while apocarotene dialdehydes with chain lengths higher than C_{10} were not detected.

Continued oxidative cleavage of apocarotene dialdehydes results in further truncation of the carotenoid backbone, generating methylglyoxal and glyoxal as terminal oxidation products, as already observed in *PSY*-overexpressing calli (Schaub et al., 2018). Similarly, in β-carotene accumulating Arabidopsis roots, methylglyoxal increased slightly whereas glyoxal levels increased two- to three-fold (Figure 2C). Gas chromatography–mass spectrometry (GC–MS) analysis of volatile, cyclic β-carotene degradation products like β-cyclocitral, β-ionone, and 5,6-epoxy-β-ionone revealed relative increases by up to factor of 15 compared to WT roots (Figure 2D).

Carotenoid pathway intermediates like phytoene, phytofluene, and ζ-carotene were not detected in WT roots. β-Apocarotenoids, apocarotene dialdehydes, and volatile cyclic β-apocarotenoids were detected in WT roots, although in very low amounts (Figure 2A). This indicates a constitutive β-carotene background breakdown even when β-carotene is barely detectable.

To identify metabolic processes altered in response to the drastically increased abundance of β-carotene and its degradation products, we analyzed the transcriptomic responses in Arabidopsis roots by RNA sequencing. The two lines *At12* and *At22* were used and compared to WT roots, each with three biological replicates. An average of 66 (WT), 65 (*At12*), and 85 (*At22*) million reads were obtained with 94% of read positions exhibiting quality scores above 30. The gene expression profile indicated highly significant changes in expression at a cutoff false discovery rate (FDR)-value of 0.05. Selection of differentially expressed genes (DEGs) with at least two-fold/four-fold changes in their expression revealed 4,000/1,217 and 3,029/866 differentially regulated genes for *At12* and *At22*, respectively, with 2,418/654 genes commonly affected in both lines. Raw RNA-Seq data were uploaded to the European Nucleotide Archive (http://www.ebi.ac.uk/ena/) under accession number ERP122176.

In-depth evaluation of transcriptome responses toward β-carotene accumulation

Although *PSY*-overexpression results in the expected phytoene accumulation, the highest relative increase compared with WT roots was observed for β-carotene (Figure 2A), indicating strongly increased phytoene conversion. Possibly, downstream carotenoid pathway enzymes involved in desaturation and isomerization of phytoene to β-carotene were induced in response to the increased phytoene supply. It has been suggested from other systems that very high carotenoid pathway activity exerts upstream feedback regulation on enzymes of the MEP pathway, which is involved in carotenoid precursor supply (Lois et al., 2000; Rodríguez-Concepción et al., 2001; Carretero-Paulet et al., 2006; Nogueira et al., 2013).

However, the RNA-Seq data analysis revealed genes of the MEP pathway were only slightly upregulated (up to 1.5-fold compared to WT roots, see Supplemental DataSet S1; Figure 3), while transcript levels of genes involved in carotene desaturation, isomerization, and cyclization (*PDS*, *ZDS*, *CrtISO*, *Z-ISO*, and lycopene cyclases) remained unaffected. Three of the four carotene hydroxylases present in the Arabidopsis genome were upregulated (*LUT1*, *BCH1*, and *BCH2*), as depicted in Figure 3 (Tian et al., 2003; Kim et al., 2009). Remarkably, expression levels of geranylgeranyl pyrophoshate synthases (GGPS) were up to eight-fold

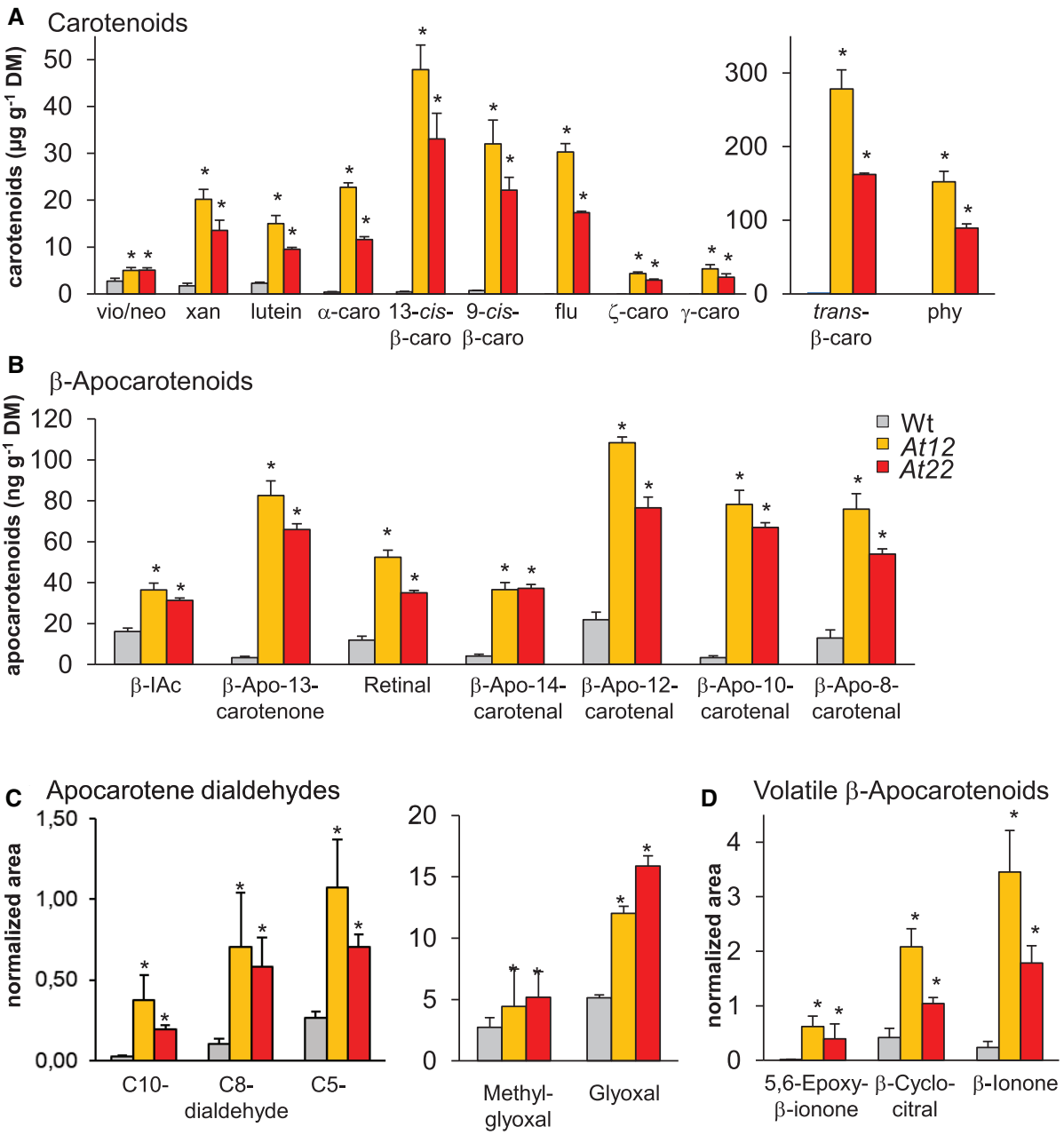

Figure 2 Carotenoids and apocarotenoids in *PSY*-overexpressing roots. Carotenoids (**A**), β-apocarotenoids (**B**), apocarotene dialdehydes (**C**), and volatile cyclic β-apocarotenoids (**D**) accumulating in roots of Arabidopsis WT and two lines with increased carotenoid pathway activity achieved through *PSY*-overexpression (*At12*, *At22*). Carotenoids and nonvolatile oxidation products (β-apocarotenoids; apocarotene dialdehydes) were analyzed by HPLC and LC–MS, whereas volatile oxidation products were analyzed by GC–MS. Results are mean ± SD from at least three biological replicates. Significant difference to the wild-type, Student's *t* test, $^{*}P < 0.05$. Volatile apocarotenoids and apocarotene–dialdehydes are expressed as peak areas normalized to internal standards and dry mass. vio/neo, violaxanthin + neoxanthin; xan, other xanthophylls; caro, carotene; flu, phytofluene; phy, phytoene; b-IAc, β-ionylidene acetaldehyde.

downregulated. The root-abundant isoforms *GGPS6*, *8*, *9*, and *10* were downregulated in *PSY*-overexpressing roots (for *GGPS10* as an example, see Figure 3), while *GGPS11*, which is highly abundant in almost all tissues except for roots, remained unaffected (Beck et al., 2013; Ruiz-Sola et al., 2016a, 2016b; Camagna et al., 2019). In conclusion, the capacity of the carotene desaturation/isomerization system is apparently sufficient to efficiently convert increased levels of phytoene formed by *PSY* overexpression into the high levels of β-carotene observed (Figure 2A). This is in line with PSY being regarded as the rate-limiting enzyme of carotenoid biosynthesis (von Lintig et al., 1997; Maass et al., 2009). The downregulation of the root *GGPS*s may represent a mechanism to limit the pathway flux.

Notably, the expression levels of *CCD1* and *CCD4* remained unaffected (Gonzalez-Jorge et al., 2013; Lätari et al.,

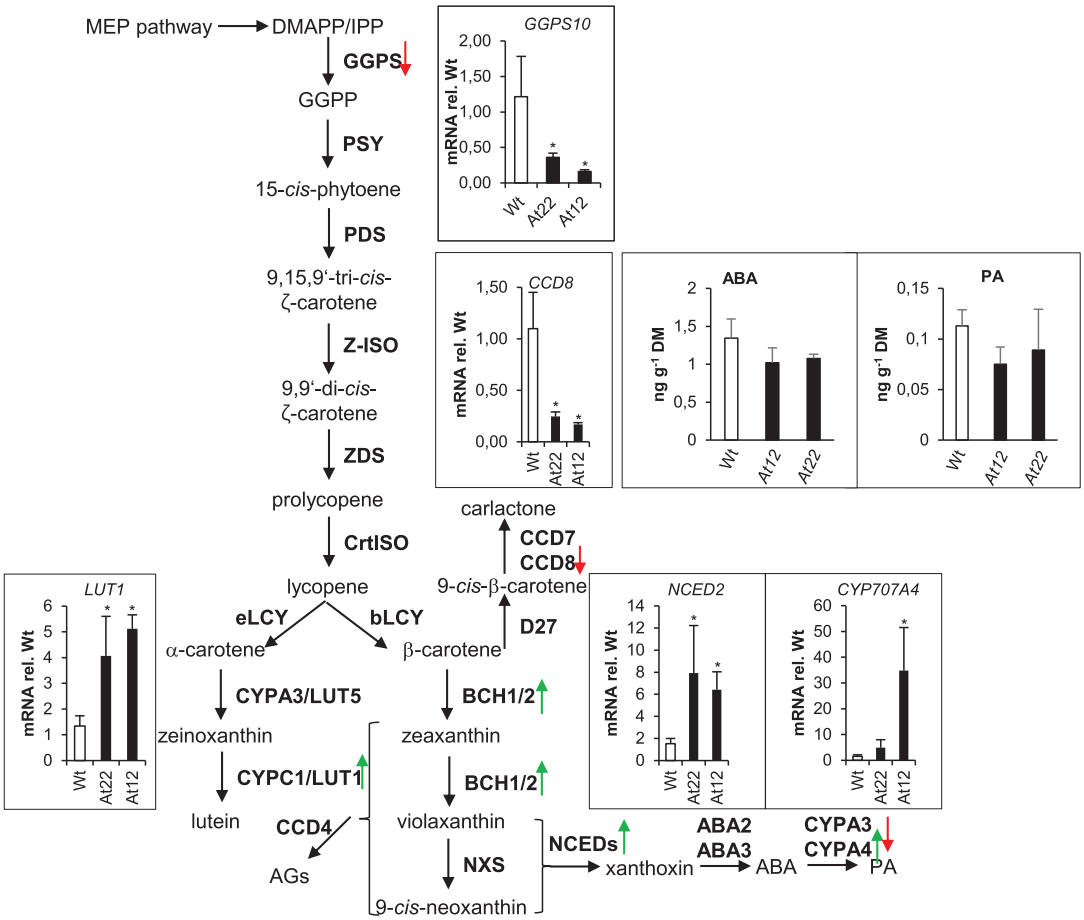

Figure 3 Transcript response of carotenogenic enzymes to β-carotene and β-apocarotenoid accumulation. Enzymes (in bold) and intermediates of carotenoid biosynthetic pathway. Trends of expression changes in response to increased β-carotene and apocarotenoid formation achieved through *PSY*-overexpression are marked with green (induction) and red (repression) arrows. Absence of arrow indicates unchanged expression levels (FDR cutoff = 0.05; at least 2-fold differences). Inset diagrams show transcript levels of selected genes in two lines (*At22*, *At12*) relative to wild-type levels, determined by RT-qPCR. ABA and PA levels were determined by LC–MS from wild-type, *At12* and *At22* roots. Results are mean ± SD from at least three biological replicates. Significant difference to the WT, Student's *t* test, $^{*}P < 0.05$. eLCY, ε-cyclase; bLCY, β-cyclase; LUT5, cytP450 hydroxylase 97A3; LUT1, cytP450 hydroxylase 97C1; BCH1/2, β-carotene hydroxylase 1/2; NXS, neoxanthin synthase; NCED, 9-*cis*-epoxycarotenoid dioxygenase; D27, β-carotene isomerase; ABA 2/3, short-chain dehydrogenase/reductase, CYPA3/A4, ABA hydroxylase.

2015; Figure 3). In contrast, only two carotenoid cleavage enzymes involved in phytohormone synthesis were differentially regulated: the transcript level of *NCED2*, involved in ABA biosynthesis, was five-fold higher while it was four-fold lower for *CCD8*, which is involved in SL biosynthesis. Moreover, two ABA hydroxylases, contributing to conversion of ABA into physiologically only weakly active hydroxy-ABA and phaseic acid (PA), were affected with opposed trends: while *CYP707A3* was downregulated, *CYP707A4* was upregulated, both with an about four-fold difference to WT roots (Dong et al., 2014). These results might suggest alterations in ABA, PA, and/or SL levels upon carotenoid accumulation in Arabidopsis roots. However, a metabolic drain of excess carotenoids into the biosynthesis of carotenoid-derived phytohormones appears unlikely to serve as a homeostatic control mechanism, considering the substantial general physiological impact this would exert. This is supported by the fact that the levels of both ABA and its major degradation product PA, as determined by LC–MS, remained unchanged in *PSY*-overexpressing roots (Figure 3).

To identify genes responding to the accumulation of β-apocarotenoids, the transcriptome data were functionally classified. Common DEGs of *At12* and *At22* roots with at least two-fold change compared to WT roots were used for gene ontology (GO) classification with the PANTHER tool (Mi et al., 2013). A GO enrichment analysis was performed to identify functional categories and processes overrepresented in response to β-carotene accumulation and to provide insight into response mechanisms. The major functional categories with a $P < 0.05$ are shown in Figure 4 (for a complete list, see Supplemental DataSet S2). DEGs with higher transcript abundance belonged to the molecular function "carbohydrate transporter activity" (overrepresented by factor 5.6) and "oxidoreductase activity" (1.8-fold) and to the biological processes "carbohydrate transport" (4.4-fold) and "ion transport" (3-fold; Figure 4, A and B,

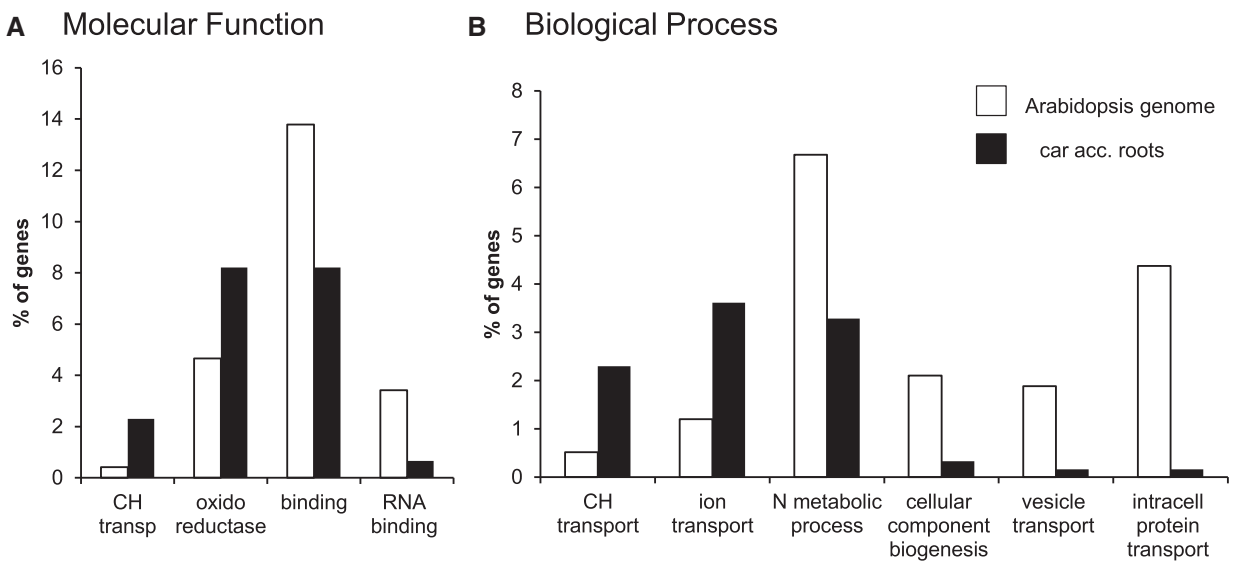

Figure 4 Functional classification of DEGs from carotenoid accumulating roots. DEGs from *PSY*-overexpressing, carotenoid-accumulating Arabidopsis roots with at least 2-fold differences to WT levels were functionally classified using the PANTHER tool. The percentage of genes from the Arabidopsis genome associated with a molecular function (**A**) and biological process categories (**B**) was used to compare the corresponding percentage of DEGs from carotenoid accumulating roots associated with the same categories. Changes in abundance indicate that the corresponding process might be affected.

respectively). DEGs with reduced transcript abundance belonged to the molecular functions "binding"/"RNA binding" (0.6-fold and <0.2-fold) and to the biological processes "nitrogen (N) compound metabolic process" (0.5-fold), "cellular component biogenesis", "vesicle-mediated transport", and "intracellular protein transport" (all <0.2-fold). The overrepresented categories might point toward further apocarotenoid metabolization by oxidoreductases and intercompartmental transportation processes of the derivatives.

Transcriptome changes are not caused by prooxidative, carotenoid-induced lipid stress response

We hypothesized that potential metabolization processes might originate from the well-known prooxidative properties of β-carotene at high oxygen partial pressure (McNulty et al., 2007). This can result in β-carotene peroxyl radicals, which generate β-carotene-lipid adducts in secondary reactions with membrane lipids (Yanishlieva et al., 1998; Wu et al., 1999). This causes lipid peroxidation through reactive chain-propagating radicals. To determine whether transcriptome changes observed in β-carotene accumulating roots are caused indirectly by lipid stress responses, we accessed a transcriptome dataset obtained upon addition of the oxylipins phytoprostane A1 (PPA1) and 12-oxo-phytodienoic acid (OPDA). Both oxylipins are formed by lipid peroxidation and are considered major signaling molecules mediating responses to lipid stress (Mueller et al., 2008). This revealed that only 7.6% (30 from 393) and 6.6% (85 from 1,293) of DEGs in OPDA- or PPA1-treated roots were differentially expressed in *At12* and *At22* roots (Figure 5A).

For further evaluation, we also determined the levels of lipid hydroperoxides and hydroxylated fatty acids as markers for lipid stress (Mosblech et al., 2009). Lipid hydroperoxides in roots of hydroponically grown plants were determined using the ferrous oxidation of xylenol orange (FOX) assay (DeLong et al., 2002; Figure 5B). As positive control, lipid hydroperoxide formation was induced by the addition of *tert*-butyl hydroperoxide (BuOOH) to WT plants (Triantaphylidès et al., 2008). While BuOOH-treated roots accumulated lipid hydroperoxides, their amounts were unchanged in nontreated carotenoid-accumulating roots. For confirmation, the patterns of hydroxylation products of the fatty acid octadecatrienoic acid (18:3; hydroxy-octadecatrienoic acid, HOTE; Sattler et al., 2006) were determined in roots from WT and *PSY*-overexpressing line *At22* by LC–MS (Figure 5C). Similar to other nonphotosynthetic tissues with low formation of $^1O_2$, WT roots accumulated low levels of $^1O_2$-specific 10- and 15-HOTE regioisomers, while those of other isomers (9-, 12-, 13-, and 16-HOTEs) generated through radical catalysis were accordingly higher (Triantaphylidès et al., 2008). Quantitation revealed that HOTEs and lipid hydroperoxide levels in carotenoid-accumulating roots were identical to the WT. Moreover, expression of two marker genes indicative of lipid stress, OPDA reductase (*OPR1*) and the cytochrome P450 enzyme *CYP81D11*, were strongly induced in BuOOH-treated roots (Stotz et al., 2013) but remained unaffected in carotenoid-accumulating roots (Figure 5D). Thus, the transcriptome changes observed upon carotenoid accumulation are not caused by carotenoid-initiated lipid stress.

We searched for similarities with putatively related responses among available transcriptome data, albeit mainly

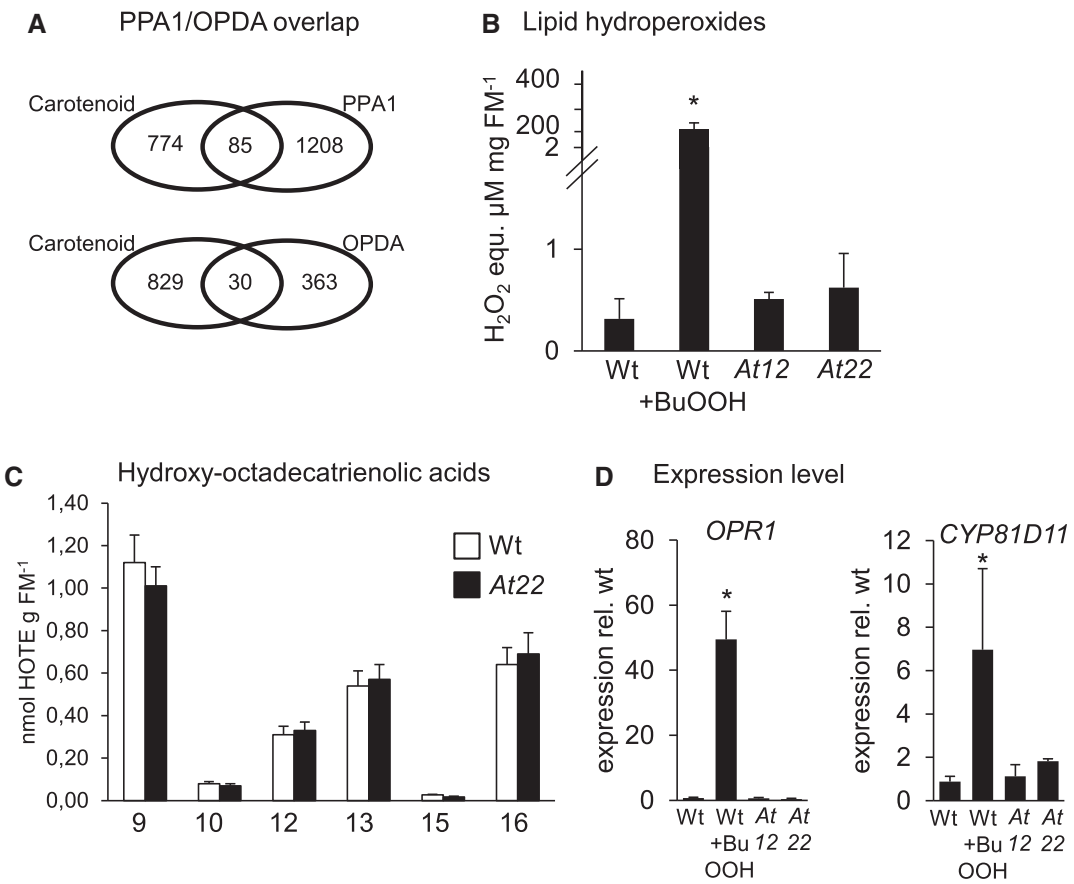

Figure 5 Lipid hydroperoxides in Arabidoposis roots. (**A**) Venn diagrams showing the overlap between commonly regulated DEGs in roots of *PSY*-overexpressing lines *At12* and *At22* (Carotenoid) and genes regulated by treatment with the oxylipins PPA1 and OPDA, respectively. (**B**) Total lipid hydroperoxides in roots from wild type, *At12* and *At22*. WT was treated with 100-mM BuOOH for 4 h to induce lipid peroxidation. Lipid hydroperoxide levels were determined with the FOX2 assay and are given in H_2O_2 equivalents per mg fresh mass (FM). Data are mean ± SD from three biological replicates. Significant difference, Student's *t* test, $^*P < 0.05$. (**C**) HOTE isomer pattern in Arabidopsis roots. The number indicates the position of the hydroxy group. 10- and 15-HOTEs are specifically formed by $^1O_2$ and accordingly low in (non-photosynthetic) roots while 9-, 12-, 13-, and 16-HOTEs are generated through both $^1O_2$ and free radical catalysis. Similar HOTE patterns in WT and carotenoid-accumulating roots (line *At22*) indicate that lipid oxidation can be excluded in transcriptome responses observed. Data are means ± SEM from nine biological replicates each. HOTEs are given in nmol g^{-1} fresh mass (FM). (**D**) Expression level of lipid stress marker genes for OPR1 and the cytochrome p450 enzyme CYP81D11. Transcripts were normalized to 18S rRNA levels and are expressed relative to levels in untreated WT. Data are mean ± SD from three biological replicates. Significant difference, Student's *t* test, $^*P < 0.05$.

available for green tissues and thereby constraining direct comparisons (Figure 6A). For instance, the carotenoid oxidation product β-cyclocitral is reported to be generated upon high light intensities and high singlet oxygen levels in leaves and to exhibit a signaling function in Arabidopsis roots (Ramel et al., 2012b; D'Alessandro et al., 2018; Dickinson et al., 2019; Felemban et al., 2019). However, only a low rate of 5.4% (62 of 1,145) of all DEGs affected by β-cyclocitral was similarly affected in carotenoid-accumulating roots of *At12* and *At22* (Supplemental DataSet S3).

The biochemical properties of the primary β-carotene oxidation products were considered for the interpretation of the transcriptome data. Most β-apocarotenoids contain a terminal carbonyl linked to an α,β-unsaturated double bond (see Figure 1). Such electrophilic carbonyls can be attacked by nucleophilic compounds, thus representing RES (Farmer and Davoine, 2007; Farmer and Mueller, 2013; Havaux, 2013). RCS, representing a subgroup of RES from fatty acid metabolism and structurally similar to apocarotenoids, cause severe cell damage and evoke distinct detoxification responses (Yamauchi et al., 2015; Mano et al., 2019a). Transcriptome changes induced by the treatment with the RCS malondialdehyde and methylvinyl ketone revealed only about 5% and 2.5% of DEG overlap with the response to β-apocarotenoid formation, respectively (Weber et al., 2004; Figure 6A). As the detoxification mechanisms for RES largely overlap with those for xenobiotics (Ramel et al., 2012c), we included datasets generated from xenobiotic-treated plants, which showed larger overlaps with DEGs for carotenoid-accumulating roots of *At12* and *At22*. For instance, patterns observed upon treatment with the allelochemical benzoxazolin-2(3H)-one and polycyclic aromatic

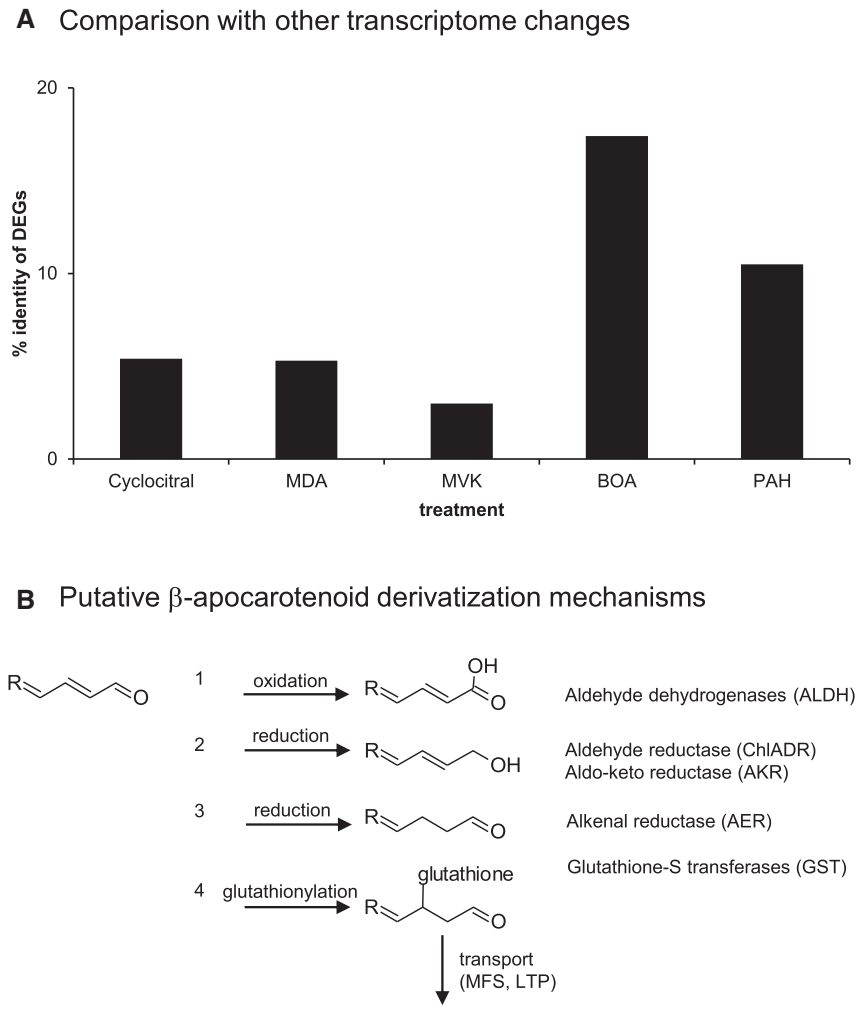

Figure 6 Metabolization of β-apocarotenoids in carotenoid-accumulating roots. (**A**) Comparison of DEGs from *AtPSY*-overexpressing roots with other transcriptome changes: treatment with the β-carotene oxidation product cyclocitral, with the RCS compounds malondialdehyde (MDA) and methyl vinyl ketone (MVK) and the allelochemical benzoxazolin-2(3H)-one (BOA) and polycyclic aromatic hydrocarbons (PAH). (**B**) Putative β-apocarotenoid derivatization mechanisms. A generalized molecule representing an unsubstituted β-apocarotenal or apocarotene-dialdehyde is shown on the left side. Possible mechanisms to reduce high reactivity of the carbonyl moiety include (1) oxidation to carboxylic acid, (2) reduction to primary alcohols, and (3) reduction of the allylic double bond, as well as with the Cys residue of glutathione (4). Proteins capable of catalyzing the corresponding reaction upregulated in carotenoid accumulating roots are given on the right side. Reactions are modified according to Grimsrud et al. (2008).

hydrocarbons showed 18 and 11% identity, respectively (Baerson et al., 2005; Weisman et al., 2010). This might indicate that the accumulation of β-apocarotenoids evokes response pathways that are similar to those observed upon xenobiotic detoxification and partially to those observed upon RES/RCS accumulation.

Genes of RCS detoxifying enzymes are induced upon β-carotene accumulation despite the absence of lipid stress

The detoxification of xenobiotic carbonyl compounds includes enzymatic reactions which reduce their reactivity, often followed by conjugation and a gain in hydrophilicity allowing their compartmentalization into vacuoles and/or excretion and storage in the cell wall (Sandermann, 1992). We considered similar reactions for β-apocarotenoids (Figure 6B) and the 100 most strongly upregulated DEGs in carotenoid-accumulating roots with at least two-fold difference were inspected (Supplemental DataSet S4) and associated with processes described for xenobiotic detoxification (Table 1). The induction of selected genes was confirmed by quantitative revese transcription PCR (RT-qPCR; see Supplemental Figure S1).

A number of defensin-like proteins associated with pathogen response were upregulated to 1,000-fold in carotenoid-accumulating roots, as well as late embryogenesis abundant proteins exhibiting protein and lipid-protective functions during oxidative and abiotic stress (Amara et al., 2014). Similarly, upregulated DEGs were associated with cell redox homeostasis, e.g. thioredoxins and glutaredoxins, while others were associated with cell wall reorganization, protein kinases, and transcription factors (Darley et al., 2001).

Table 1 Strongly induced DEGs in carotenoid-accumulating Arabidopsis roots

Locus ID	Name	loc	Description	Function	Fold change	
					At22	*At12*
Transporters						
AT2G18590		**P**	**MFS superfamily protein**	**CH transport**	**21**	**160**
AT4G12500	**LTP3**	**EC**	**Lipid transfer protein 3**	**Lipid transport**	**31**	**138**
AT1G66570	SUC7	PM	Sucrose transport protein, MFS family	CH transport	38	98
AT3G57310		EC	Lipid transfer protein	Lipid transport	27	41
AT2G18480	PLT3	PM	Polyol transporter 3, put, MFS family	CH transport	12	25
Cell wall reorganization						
AT2G43890		ER	Pectin lyase-like protein	Pectin degradation	397	2415
AT4G37990	**CAD8**	**CP**	**Cinnamyl alcohol dehydrogenase 8**	**Lignin biosynthesis**	**293**	**206**
AT2G05520	GRP3	EC	Glycine-rich protein 3	Cell size regulation	74	188
AT4G24000	CSL2	PM	Cellulose synthase-like protein G2	Cell wall	147	184
AT5G07430		EC	Pectin lyase-like protein	Pectin degradation	222	72
AT1G67980	CCAOMT	CP	Caffeoyl-CoA O-methyltransferase, put.	Lignin biosynthesis	27	22
AT3G49120	PRX34	EC	Peroxidase 34	Ox. burst/lignin	17	76
AT5G05340	PRX52	EC	Peroxidase 52	Ox. burst/lignin	75	27
Pathogen response						
AT1G19610	**PDF1.4**	**EC**	**Defensin-like protein 19**	**LCR78**	**669**	**1576**
AT3G59930		EC	Defensin-like protein 206		30	1013
AT3G61172	LCR8	EC	Defensin-like protein 128		67	423
AT5G33355		EC	Defensin-like protein 207		12	403
AT4G29305	LCR25	EC	Defensin-like protein 159		55	139
AT2G43510	TI1	EC	Defensin-like protein 195	Trypsin inhibitor	89	55
AT2G02120	PDF2.1	EC	Defensin-like protein 4	Peptidase inhibitor	18	34
Metabolic enzymes						
AT5G24160	**SQE6**	**ER**	**Squalene epoxidase 6**	**Sterol bios.**	**231**	**707**
AT3G49620	**DIN11**	**CP**	**2-Oxoacid-dependent dioxygenase**	**Many substrates**	**65**	**93**
AT4G22753	SMO1-3	ER	Methylsterol monooxygenase 1-3	Sterol/FA biosynth.	27	60
AT5G23010	MAM1	P	Methylthioalkylmalate synthase 1	Glucosinolate bios.	50	55
AT2G25450		CP	2-Oxoacid-dependent dioxygenase	Glucosinolate bios.	32	45
AT5G16970	**AER**	**CP**	**NADP-dependent alkenal reductase P1**	**Carbonyl detox.**	**25**	**42**
AT2G38240		CP	2-Oxoacid-dependent oxygenase		105	32
AT1G80160	GLYI7	CP	Lactoylglutathione lyase/glyoxalase I	Aldehyd detox.	10	29
AT5G24210		?	Alpha/beta-hydrolase	Triglyceride lipase	37	44
AT3G04000	**ChlADR**	**P**	**NADP-dependent aldehyd reductase**	**Carbonyl detox.**	**5**	**6**
Oxidation-reduction process/cell redox homeostasis						
AT3G26190	CYP71B21	EC	Cytochrome P450		42	32
AT3G15840	PIFI	P	Post-illumination chlorophyll fluorescence increase		22	56
AT3G56350	SOD	M	Superoxide dismutase	O_2^- detox.	49	43
AT4G15690	**GRXS5**	**CP**	**Monothiol glutaredoxin-S5**	**Thioredoxin**	**154**	**675**
AT4G15670	GRXS7	CP	Monothiol glutaredoxin-S7	Thioredoxin	14	55
AT2G47870	ROXY5	CP	Glutaredoxin-C12	Glutaredoxin	32	36
AT3G09270	GSTU8	CYT	Glutathion S transferase	Glutathionyl	6	10
AT4G31870	GPX7	P	Glutathione peroxidase 7	H_2O_2 detoxification	10	10
Protection against oxidative stress						
AT1G52690	LEA7	CP	Late embryogenesis abundant protein		42	66
AT2G41280	M10	CP	Late embryogenesis abundant protein M10		24	49
AT5G44310		P	Late embryogenesis abundant protein		14	25
AT3G17520		ER	Late embryogenesis abundant protein		68	21
Protein kinases/regulatory proteins						
AT1G29090		CP	C1A cysteine proteinases superfamily		94	696
AT2G29930		N	F-box/RNI-like/LRR2 protein		35	624
AT1G51820		PM	LRR receptor-like S/T-protein kinase		80	494
AT4G05380		PM	P-loop nucleoside triphosphate hydrolase		61	204
AT2G27535	RPL10A	CP	Ribosomal protein L10A family protein		38	194
AT5G43570		PM	Serine protease inhibitor	PR peptide	122	91
AT2G05430		N	Ubiquitin-specific protease C19-related		36	84
AT4G29970		N	F-box protein, putative		38	56
AT5G43580	UPI	EC	Serine protease inhibitor	PR peptide	31	37
AT1G35750	APUM10	CP	Pumilio homolog 10, putative	RNA regulation	6	32

(continued)

Table 1 Continued

Locus ID	Name	loc	Description	Function	Fold change	
					At22	*At12*
Transcription factors						
AT4G28140	ERF054	N	ERF/AP2 transcription factor, DREB A-6		85	97
AT3G02150	PTF1	N/P	Plastid transcription factor 1, teosinte branched1		15	59
Hormone biosynthesis						
AT4G13260	YUC2	N	IPA monooxygenase YUCCA2	Auxin	97	83
AT3G19270	CYP707A	PM	Abscisic acid 8′-hydroxylase 4	ABA	5	37
AT3G63110	IPT3	N/P	Adenylate isopentenyltransferase 3	Cytokinin	7	23
AT1G30040	GA2OX2	CP	Gibberellin 2-beta-dioxygenase 2	C-19 GAs	8	19

CCAOMT, caffeoyl-CoA O-methyltransferase; CSL2, cellulose-synthase like protein. RNA Seq-determined expression changes in roots of *PSY*-overexpressing lines *At22* and *At12* relative to WT roots for genes selected from the 100 DEGs with highest induction levels. The predicted localization is indicated by CP, cytoplasm, EC, extracellular, P, plastid, M, mitochondria, PM, membrane system, N, nucleus; expression changes for genes in bold were confirmed by RT-qPCR (see Supplemental Figure S1).

The partial overlap in the response of *At12* and *At22* with the response to treatments with RES and xenobiotic detoxification reactions prompted us to screen for candidate genes/enzymes capable of lowering the reactivity of β-apocarotenoids. We focused on enzymes involved in carbonyl detoxification at small to medium chain hydrocarbon residues, similar to β-apocarotenoids (Mano et al., 2019b). Interestingly, the plastid-localized nicotinamide adenine dinucleotide phosphate (NADPH)-dependent aldehyde reductase ChlADR, mediating the reduction of aldehyde/ketone functions to hydroxyl functionalities (Yamauchi et al., 2011), was induced up to six-fold in *At22* and *At12* (Supplemental Figure S1). Moreover, the NADPH-dependent aldo-keto reductases AKR4C8 and AKR4C9, also mediating reduction to alcohols, were induced by about 2.2- and 10.1-fold, respectively. Furthermore, the NADPH-dependent 2-alkenal reductase (AER), reducing allylic α,β-unsaturated double bonds while maintaining the aldehyde function (Mano et al., 2005; Yamauchi et al., 2011), was induced 25- and 42-fold, respectively. Remarkably, the induction rate was higher in *At12* than in *At22* for these enzymes, corresponding to the event-specific differences in β-apocarotenoid levels. Oxidation into carboxylic acids by aldehyde dehydrogenases represents another detoxifying redox reaction (Stiti et al., 2011a). An aldehyde dehydrogenase in *Synechocystis* sp. PCC6803 not only converts aliphatic hydrocarbon aldehydes, but also β-apocarotenals into β-apocarotenoic acids in vitro (Trautmann et al., 2013). Its closest Arabidopsis homologs, namely ALDH3H1 and ALDH3I1, were induced slightly in *At12* and *At22* but below two-fold (Supplemental DataSet S4). They are known to detoxify short and medium chain hydrocarbon aldehydes by oxidation in vitro (Stiti et al., 2011a), whereas their activity on β-apocarotenoids remains to be investigated.

RCS detoxifying enzymes also modify and detoxify β-apocarotenoids

We performed in vitro assays with purified recombinant enzymes from ChlADR, AKRC8, AKRC9, AER, ALDH3H1, and ALDH3I, using all primary β-apocarotenals as substrates to investigate whether these enzymes are capable of metabolizing β-apocarotenoids. Activity was analyzed by high-performance liquid chromatography-diode array-detection (HPLC-DAD) and products formed were further characterized by LC–MS and gas chromatography-mass spectrometry (GC-MS). See Supplemental Table S1 for detailed information on enzyme activities and Figure 7 as an overview on substrate specificities.

The 2-alkenal reductase AER was capable of forming dihydro-β-apo-14′-carotenal, dihydro-β-apo-13-carotenone and dihydro-β-ionone from the corresponding β-apocarotenoids as substrates, as deduced from molecular masses by LC–MS analysis (Supplemental Figures S2–S3). In contrast, all other β-apocarotenoid substrates were not converted, including β-apo-8′-carotenal, β-apo-10′-carotenal, β-apo-12′-carotenal, retinal, β-apo-11′-carotenal, and β-cyclocitral, even under a variety of assay and substrate solubilization conditions (detergent micelles, addition of dimethyl sulfoxide [DMSO]).

The aldo-keto reductase AKR4C9 reduced β-apo-14′-carotenal, retinal, β-apo-11′-carotenal, and β-ionone into the corresponding alcohols β-apo-14′-carotenol, retinol, β-apo-11-carotenol, and β-ionol, respectively, and AKR4C8 reduced β-apo-11′-carotenal and β-ionone. This is supported by molecular masses determined upon LC–MS and the identical chromatographic behavior and UV/VIS spectra of reaction products with the respective apocarotenol standards (Supplemental Figures S4–S5). Recombinant ChlADR selectively converted retinal and β-apo-11-carotenal into the corresponding alcohols in vitro (Supplemental Figures S6–S8).

Both aldehyde dehydrogenases ALDH3H1 and ALDH3I1 displayed broad substrate specificity for β-apocarotenoids. They converted most of them into the corresponding carboxylic acids, as supported by molecular masses obtained by LC–MS and by the fact that the product formed from retinal corresponded to an authentic standard of all-*trans*-retinoic acid in terms of chromatographic and spectral properties (Supplemental Figures S9–S11). Exceptions were the two ketones β-apo-13-carotenone and β-ionone for which a conversion into carboxylic acids is biochemically impossible, and ALDH3H1 did not convert β-apo-8-carotenal and retinal. Remarkably, however, β-cyclocitral remained unmetabolized.

The apocarotene dialdehyde apo-8,8′-carotene-dial, which can be formed from β-carotene, α-carotene, as well as from

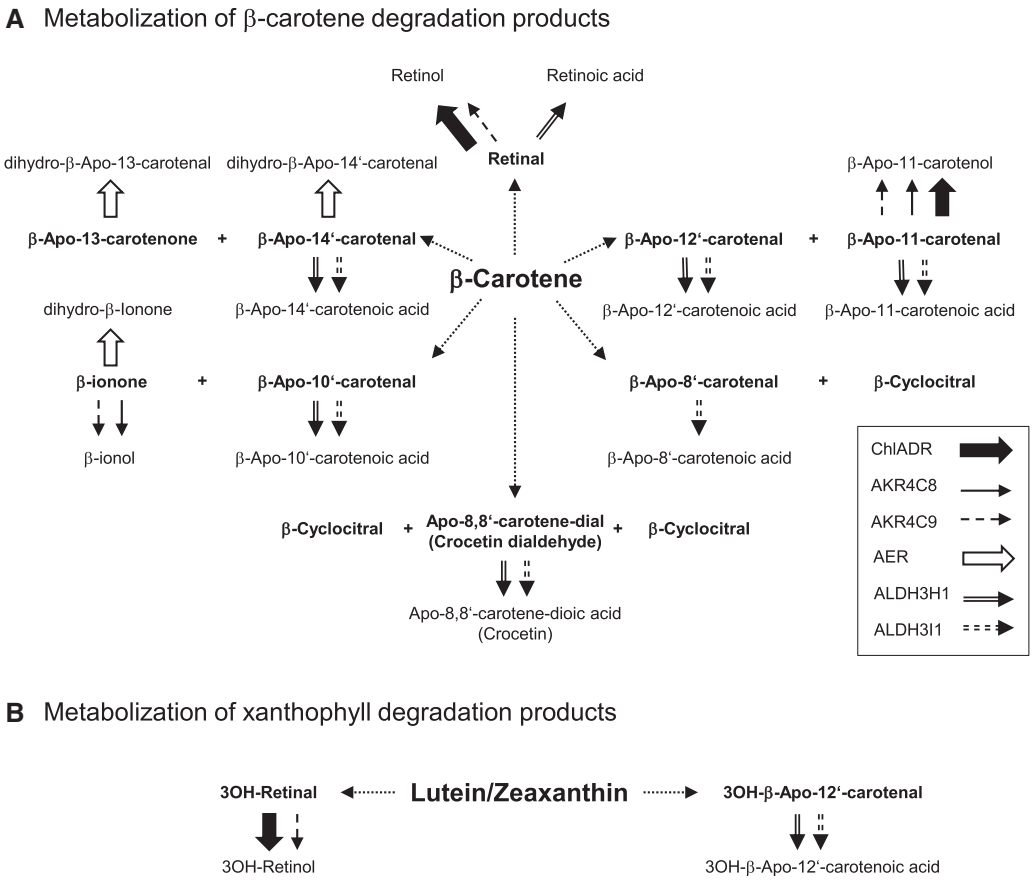

Figure 7 Overview on β-apocarotenal, xanthophyll, and carotene-dial conversion by carbonyl-detoxifying enzymes. Metabolization of primary oxidation products generated from β-carotene (**A**) and lutein and zeaxanthin (**B**) as exemplary xanthophylls. Arrows indicate whether enzymatic reduction into alcohols (ChlADR, AKR4C8, AKR4C9), oxidation into apocarotenoic acids (ALDH3H1 and ALDH3I1) or reduction into dihydro-apocarotenals (AER) was observed in in vitro assays. Complete number of products generated upon oxidation of each possible backbone double bond is shown for β-carotene only.

xanthophylls, was metabolized into apo-8,8′-carotene-dioic acid, known as the major saffron pigment crocetin (Supplemental Figure S10G). ALDHs might therefore additionally participate in the detoxification of primary xanthophyll cleavage products. We therefore tested xanthophyll-derived 3′-hydroxylated apocarotenals as substrates. Using 3-OH-retinal and 3-OH-β-apo-12′-carotenal as exemplary substrates for short and long-chained hydroxylated carotenoids, we found that both ChlADR and AKR4C9 generated 3-OH retinol, while both ALDH enzymes generated the corresponding carotenoic acid from 3-OH-β-apo-12′-apocarotenal (Supplemental Figure S10H). These results extend the possible range of detoxification activity of these enzymes to xanthophyll degradation products.

Discussion

Apocarotenoid metabolism shows similarities to reactive carbonyl species and xenobiotic detoxification

High concentration of β-carotene achieved by pathway engineering is sufficient for the formation of β-carotene crystals in nongreen tissues like Arabidopsis roots and callus (Álvarez et al., 2016; Schaub et al., 2018). Likewise, carotenoids are predominantly deposited as crystals in tissues of plants considered as "natural" carotenoid accumulators, e.g. in carrot (*Daucus carota*) roots, pumpkins (*Cucurbita pepo*), orange cauliflower (*Brassica oleracea* var. *botrytis*), and melons (*Cucumis melo*; Ben-Shaul and Naftali, 1969; Paolillo et al., 2004; Maass et al., 2009; Jeffery et al., 2012; Schweiggert et al., 2012). However, even when crystals are present, β-carotene is subjected to nonenzymatic oxidation yielding β-apocarotenoids (Schaub et al., 2018). Nonenzymatic oxidation accounts for substantial provitamin A losses in crops, fruits, and vegetables e.g. maize (*Zea mays*) grains (Taleon et al., 2017) and provitamin A-biofortified Golden Rice (*Oryza sativa*; Beyer et al., 2002; Schaub et al., 2017). Remarkably, β-carotene losses during rice endosperm development yield only low amounts of β-apocarotenoids of various chain lengths, while the vast majority of β-carotene is autoxidized to form carotenoid-oxygen copolymers (Schaub et al., 2017). Such copolymers form in a variety of plant tissues and are quite resistant toward further decomposition (Burton et al., 2016). In contrast to starchy rice and maize endosperm consisting of dead cells generated via programmed cell death (Young and Gallie,

2000) and fruits as dying organs, living plant cells need to prevent β-carotene autoxidation and concomitant cytotoxic effects. This requires efficient, coordinated control over both carotenoid biosynthesis and degradation. Degradation is expected to involve well-coordinated metabolization of the primary oxidation products, namely β-apocarotenoids, via yet unknown metabolic paths.

The transcriptomes of *At12* and *At22* roots accumulating β-apocarotenoids share overlaps with those of plants treated with xenobiotics and various RCS (Figures 5 and 6A). This suggests utilization of common detoxification and metabolization mechanisms for xenobiotics, RCS and β-apocarotenoids. Apocarotenoids and RCS are lipophilic hydrocarbons of aliphatic and/or cyclic structure and contain aldehyde or ketone functionalities. Importantly, β-apocarotenoids are α,β-unsaturated carbonyls like RCS and their toxicity originates from their reactivity with thiol and amino groups (Yamauchi et al., 2011).

The detoxification of RCS and xenobiotics has been investigated in plants, and a three-phased model has been proposed for xenobiotics (for review, see Sandermann, 1992). It comprises (I) transformation of (mostly lipophilic) xenobiotics into more soluble derivatives, (II) conjugation, e.g. to glutathione or sugar moieties, and (III) compartmentalization and storage into vacuoles, the apoplast or cell wall components. Conjugated xenobiotics are stored in vacuoles when hydrophilic or, after transporter-mediated export, in the cell wall when hydrophobic.

Research on RCS detoxification in plants has revealed a diverse set of NADPH-dependent, RCS-reducing enzyme activities (for review, see Mano, 2012), which can be considered as phase I enzymes. These enzymes detoxify a wide range of RCS substrates by reducing either aldehyde/ketone into hydroxyl functionalities (aldo-keto reductases AKR4C8 and AKR4C9, Simpson et al., 2009; aldehyde reductase ADR, Yamauchi et al., 2011). Alternatively, the α,β-unsaturated C–C double bonds are saturated by the 2-alkenal reductase AER (Mano et al., 2005) and the alkenal/-one oxidoreductase AOR (Yamauchi et al., 2012).

Early-phase modification of apocarotenoids by enzymes related to RCS detoxification

Considering similarities between apocarotenoids and RCS, we searched for induced RCS detoxifying enzymes in the transcriptomes of *At12* and *At22* roots assuming their substrate specificities might also allow the conversion of β-apocarotenoids. RCS detoxification enzymes, namely AKR4C8 and AKR4C9, ADR as well as AER were strongly induced (see Supplemental DataSet S4). Absence of typical markers for lipid peroxidation (Figure 5) excluded the possibility that these enzymes were induced for the purpose of lipid-breakdown product detoxification, potentially formed upon prooxidative activities of β-carotene. Instead, it is feasible to interpret their upregulation in terms of a direct response to increased carotenoid cleavage.

All four enzymes were capable of converting various intermediates of β-carotene and xanthophyll degradation in vitro. They converted β-apocarotenoids and 3-OH-apocarotenoids, the primary cleavage products of β-carotene/α-carotene and xanthophylls, respectively, as well as apocarotene dialdehydes, originating from repeated apocarotenoid cleavage. Notably, β-apo-14′-carotenal (C_{22}) was the longest-chain and β-ionone (C_{13}) the shortest-chain β-apocarotenoid converted, suggesting narrow apocarotenoid substrate specificity (Figure 7; Supplemental Table S1). Interestingly, AER reduced the α,β-unsaturated C–C double bond only of β-apo-14′-carotenal, β-apo-13′-carotenone, and β-ionone to yield by far less reactive dihydro β-apocarotenoids. These β-apocarotenoids probably represent the most reactive and potentially most cytotoxic β-apocarotenoids as methylation of the α,β-unsaturated double bond present in all other β-apocarotenoids, except for β-apo-10′-carotenal, lowers their reactivity (Figure 1). In β-apo-10′-carotenal, however, the length of the polyene system might render the double bond more inert. It might therefore be that substrate specificity of AER is adapted to detoxify these highly reactive apocarotenoids by removing the α,β-unsaturated C–C double bond (Mano et al., 2002, 2005). Previously, AER was reported to be localized in the cytosol, to be primarily expressed in leaves and to convert RCS/oxylipins as oxygenated hydrocarbons of a length up to C_{18} (Mano et al., 2005).

ADR had a very narrow substrate specificity and converted only retinal and β-apo-11′-carotenal into the corresponding carotenols. Additionally, 3-OH-retinal that might originate from nonenzymatic xanthophyll cleavage was also converted (Figure 7). ADR was previously shown to reduce saturated and α,β-unsaturated aldehydes with minimum five carbon atoms such as alkanals and alkenals and methylglyoxal in vitro (Yamauchi et al., 2011).

AKR enzymes also showed quite narrow substrate specificity (Figure 7). Both AKR4C8 and AKR4C9 reduced β-apo-11′-carotenal and β-ionone and AKR4C9 additionally reduced retinal, β-apo-14′-carotenal, as well 3-OH-retinal. Both enzymes were previously reported to exhibit broad substrate specificity in vitro accepting sugars, steroids, ketosteroids, aliphatic, and aromatic aldehydes (Simpson et al., 2009; Saito et al., 2013; Sengupta et al., 2015).

In addition to these well-known RCS detoxifying enzymes, we also considered enzymatic oxidation of β-apocarotenals into β-apocarotenoic acids by NAD^+/$NADP^+$-dependent aldehyde dehydrogenases, known to prevent RCS accumulation under abiotic stress (for review, see Stiti et al., 2011b). Notably, aldehyde dehydrogenase SynAlh (*slr0091*) from *Synechocystis* sp. PCC6803 converted not only alkanals but also β-apocarotenals into β-apocarotenoic acids in vitro (Trautmann et al., 2013) and the two closest Arabidopsis homologs, ALDH3H1 (sequence identity 43.6%) and ALDH3I1 (sequence identity 37.3%), were identified. However, ALDH3H1 and ALDH3I1 have only been reported to oxidize aliphatic alkanals (hexanal to dodecanal; C_6–C_{12}) and α,β-unsaturated aldehydes in vitro (Stiti et al., 2011a).

In fact, both Arabidopsis ALDH enzymes were capable of converting all canonical β-apocarotenals into their corresponding β-apocarotenoic acid (Figure 7), with the exception of β-cyclocitral with both enzymes and β-apo-8′-carotenal with ALDH3H1. Assuming a pK_A of approximately 4.8 as for retinoic acid, conversion into β-apocarotenoic acids does not only decrease reactivity but increases water solubility due to a deprotonated carboxylic functionality under physiological pH.

Complementing functions by β-apocarotenoid modifying enzymes and implications for xanthophyll metabolism

We noted a pattern of redundancy and also complementation in terms of localization and substrate specificity for the enzymes involved in apocarotenoid metabolism. Regarding substrate specificities, the reducing enzymes AKR, ADR, and AER mainly target shorter-chain apocarotenones, such as β-ionone and β-apo-13′-carotenone, whereas ALDHs oxidized almost all apocarotenals, including long-chain ones like β-apo-10′-carotenal (Figure 7). Additionally, the two systems complement each other as the reducing enzymes primarily target ketone substrates that cannot be oxidized biochemically, such as by ALDH. This indicates complementing functions between oxidizing and reducing enzyme systems. In terms of localization, previous findings suggest redundancy in enzyme activity localization in chloroplasts and the cytosol. ADR, AKR4C9, and ALDH3I1 are plastid-localized, whereas AER, AKR4C8, ALDH3H1 are localized in the cytosol (Mano et al., 2005; Simpson et al., 2009; Stiti et al., 2011a; Yamauchi et al., 2011). This suggests a primary activity on apocarotenoids at the site of their major formation, in plastids, while maintaining cytosolic activity as a back-up should β-apocarotenoids exit plastids by diffusion and/or export mechanisms. Interestingly, ALDH3H1 exhibited very low activity on β-apo-8′-carotenal (Figure 7), which is unlikely to exit plastids by diffusion due to its high hydrophobicity.

The only β-apocarotenoid, which was not metabolized by any of the enzymes identified, was β-cyclocitral. However, β-cyclocitral is far less reactive than other β-apocarotenoids as its double bond is stabilized by its position within the ionone ring (Figure 1). It can be nonenzymatically detoxified to β-cyclocitric acid/β-cyclogeranic acid via a Baeyer–Villiger-type oxidation in aqueous solution (Tomita et al., 2016). Notably, β-cyclocitric acid/β-cyclogeranic acid is formed nonenzymatically from β-cyclocitral, the latter accumulating upon light stress-induced, nonenzymatic β-carotene oxidation (Ramel et al., 2012a; D'Alessandro and Havaux, 2019). It has recently been reported as a potential signaling compound conferring drought resistance to plants (D'Alessandro et al., 2018).

Lastly, considering results obtained for selected 3-OH-β-apocarotenoids (Figure 7), ALDHs, ADR, and AKR might also contribute to metabolism and detoxification of these xanthophyll-specific degradation products. Turnover of xanthophylls, providing photoprotection via the xanthophyll cycle, is expected to be very high in photosynthetic tissues due to nonenzymatic processes, especially under high-light stress (Niyogi et al., 1998).

Saffron as a natural model for apocarotenoid metabolism

The red color in saffron stigma originates from crocins, a group of glucose conjugates of the apocarotenoid crocetin dialdehyde (apo-8,8′-carotene-dialdehyde) accumulating up to 10% on a dry mass basis (for review, see Ahrazem et al., 2015b; Demurtas et al., 2019). Considering the reactivity of crocetin dialdehyde with two α,β-unsaturated double bonds and carbonyl groups, efficient metabolism in *Crocus sativus* to avoid its toxicity and allow for accumulation of high crocin amounts can be assumed. These metabolic processes might represent an example of general apocarotenoid metabolism mechanisms in plants.

Interestingly, the sequence of reactions in crocetin dialdehyde metabolism in saffron strongly resembles the three-phase model of xenobiotic detoxification described above. In *Crocus* stigmas, crocetin dialdehyde is formed enzymatically in plastids via cleavage of zeaxanthin by CCD2 and thereafter oxidized by the endoplasmic reticulum membrane-associated aldehyde dehydrogenase ALDH3I1 to yield the dicarboxylic acid crocetin (Frusciante et al., 2014; Ahrazem et al., 2015a). By glycosylation of the carboxylic groups by the cytosolic UDP-glycosyltransferase (UGT) UGT74AD1 and a yet unknown cytosolic UGT, crocins are formed and then sequestered in vacuoles by active transport through ABCC2 and ABCC4a (Demurtas et al., 2018, 2019; Diretto et al., 2019). In phase I, crocetin dialdehyde is detoxified by ALDHs into the far more water-soluble dicarboxylic acid crocin. Glycosylation in phase II further increases water solubility and decreases reactivity. Compartmentalization into vacuoles in phase III allows for long-term storage and higher stability of crocin than in the cytosol (Sandermann, 1992; Demurtas et al., 2019).

Overexpression of Crocus *CCD2* in *Nicotiana benthamiana* leaves leads to the accumulation of crocins, implying the existence of endogenous ALDHs oxidizing crocetin dialdehyde to its corresponding dicarboxylic acid crocetin as well as of UGTs for subsequent glycosylation in vegetative tissues (Demurtas et al., 2018). As we show, the two Arabidopsis enzymes ALDH3H1 and ALDH3I1 are capable of performing this reaction, suggesting that these metabolic reactions might be of general importance for apocarotenoid metabolism in plants. It appears that saffron "recruited" enzymes from a primary detoxification pathway for the evolution of a biosynthesis pathway specialized for pigmentation. This involves the neofunctionalization of a CCD copy to specifically cleave zeaxanthin into crocetin dialdehyde.

Remarkably, nonenzymatic cleavage of β-carotene and xanthophylls at C8 and C8′ is a source of crocetin dialdehyde in plants, despite the lack of CCD2. This is exemplified by β-carotene accumulating *At12* and *At22* roots, where short-chain apocarotene dialdehydes, and potentially

crocetin dialdehyde, accumulate (Figure 2). Similar to saffron, we have demonstrated that ALDH3H1 and ALDH3I1 from Arabidopsis are induced in *At12* and *At22* and are capable of converting crocetin dialdeyhde into the corresponding dicarboxylic acid crocetin in vitro (Figure 7). In agreement with the glycosylation of crocetin in saffron, 11 UDP glycosyl transferases were upregulated in *At12* and *At22* roots up to 22-fold (UGTs 71B7, 73B1, 73C3, 73D1, 74C1, 76E2, 82A1, 84A4, 85A2, 88A1, and 91C1). Notably, glycosylation of xanthophyll-derived apocarotenoids exists not only in various fruits, e.g. grapes *(Vitis vinifera)* but also in Arabidopsis leaves as a compensatory mechanism for increased carotenoid flux (Winterhalter and Rouseff, 2001; Lätari et al., 2015). Accordingly, bioinformatics and homology search against the cytosolic saffron UGT74AD1, followed by functional analysis of individual UGTs, could aid in identifying UGTs potentially involved in glycosylation of β-apocarotenoic acids as wells xanthophyll-derived 3-OH-apocarotenoic acids, which can be produced by ALDH3H1 and ALDH3I1 as demonstrated in this work (Figure 7).

Transport processes and cell wall modifications might facilitate compartmentalization of apocarotenoids and their conjugates

As described above, xenobiotic conjugates are compartmentalized into the cell wall or vacuole (Sandermann, 1992) and, notably, crocins in saffron are deposited in vacuoles (Demurtas et al., 2019). Our transcriptome data provides evidence that similar transport processes might be relevant in carotenoid metabolism. A significant number of plastid and plasma membrane-localized transporters were identified in the DEGs (Supplemental Figure 3), mainly associated with transport of carbohydrates (Figure 4). Members of the ABC transporter family were induced up to eight-fold: ABCG14, ABCG21, ABCG30, ABCE1, as well as ABC2 homologs 11 and 14 (Supplemental DataSet S4). Only a few of the more than 100 ABC transporters genes have been functionally characterized and shown to be involved in detoxification, abiotic stress response, and deposition of surface wax compounds (Kang et al., 2011). However, two family members transport apocarotenoid derivatives. AtABCC2 transports ABA glucosylesters into vacuoles, resulting in their physiological inactivation (Burla et al., 2013). Notably, CsABCC2 and CsABCC4a mentioned above and involved in crocin transport in saffron (Demurtas et al., 2019) are close homologs of AtABCC2. Functional analysis, e.g. by transportomics assays, might help to identify candidate transporters induced in *At12* and *At22*, which are capable of transporting apocarotenoid metabolites (Demurtas et al., 2020). Similar to crocin metabolism in saffron (Demurtas et al., 2019), we have shown that ALDHs in Arabidopsis form apocarotenoic acids, which might be glycosylated by UGTs and transported by ABC transporters.

Another protein family of which at least half a dozen members are upregulated in *At12* and *At22* roots and that might mediate increased cellular mobility and compartmentalization of apocarotenoids are lipid transfer proteins. They are known to possess elongated, hydrophobic binding for binding medium-chain hydrocarbons and are thought to mediate lipid transport between membrane systems, deposition of wax compounds of suberin, cutin, and sporopollenin in the apoplast as well as signaling processes (for review, see Salminen et al., 2016; Edqvist et al., 2018). Given that a large proportion of nonconjugated apocarotenoids consists of a medium-chain hydrocarbon moiety (Figure 1), it appears attractive to suggest that LTPs might mediate apocarotenoid mobility between compartments or might serve as mediators of apocarotenoid signaling.

Many DEGs in *At12* and *At22* were associated with cell wall biosynthesis. Among them were pectin lyases, one cinnamyl alcohol dehydrogenase protein8, caffeoyl-CoA O-methyltransferase, one cellulose-synthase like protein, as well as two peroxidases (PRX34, PRX52) participating in lignin polymerization (Tenhaken, 2015) and induced up to 76- and 75-fold, respectively. A glycine-rich protein, induced up to 190-fold, is associated with regulation of cell wall growth (Park et al., 2001).

In line with the model of Sandermann (1992), cell wall reorganization in *At12* and *At22* roots might facilitate the apoplastic deposition of hydrophobic β-apocarotenoids derivatives as a means of detoxification. Enzymatic cell wall polymerization is known to facilitate long-term storage of hydroxylated metabolites and exploited, for instance, in phytoremedation, and there is evidence that a number of (hydrophobic) xenobiotics are transported to the cell wall where they remain covalently bound to lignins, hemicelluloses, and pectins (Harvey et al., 2002).

Retrograde signaling feedback regulates carotenogenesis upon accumulation of β-carotene and β-apocarotenoids

Carotenoid biosynthesis is assumed to involve regulatory feedback loops, coordinating nuclear transcriptional, and biosynthetic enzyme activities to achieve the appropriate amount and pattern of carotenoids (Diretto et al., 2007; Bai et al., 2009; Kachanovsky et al., 2012; Arango et al., 2014; Álvarez et al., 2016). This requires pathway-specific signal molecules derived from apocarotenoids capable in relaying information on the carotenoid status. This agrees with known mechanisms of carotenoid-derived hormone signaling such as SLs, ABA, zaxinone, and cyclocitral (Felemban et al., 2019).

Transcript analysis of carotenoid accumulating Arabidopsis roots revealed that most of the changes can be interpreted in terms of counteracting excess β-carotene accumulation. For instance, *GGPS* repression would limit supply of the carotenoid precursor GGPP and the induction of α- and β-carotene hydroxylase genes *BCH1/2* and *LUT1* aims at increasing β-carotene conversion into xanthophylls. However, these responses appear insufficient to compensate for the constitutive expression of the *PSY* transgene.

β-Apocarotenoids themselves or more water-soluble derivatives thereof appear as likely candidate molecules to perform feedback signaling as their cellular abundances could inform on the extent of nonenzymatic degradation. As we show, the enzymes ChlADR, AKR4C9, ALDH3H1, and ALDH3I1 have the potential to also convert xanthophyll degradation products. Turnover of xanthophylls, providing photoprotection via the xanthophyll cycle, is very high in photosynthetic tissues due to nonenzymatic processes intensified under high-light stress (Beisel et al., 2011; Lätari et al., 2015). In fact, the immediate nonenzymatic β-carotene cleavage product β-cyclocitral acts as a retrograde signaling molecule transferring information on photooxidative stress levels, although it is unknown whether this signaling mechanism incudes additional metabolization reactions (D'Alessandro et al., 2018). Therefore, these enzymes and their respective protein family members represent good candidates for future investigations in this direction.

We have identified enzyme systems in which transcripts were induced upon massive accumulation of β-carotene and its oxidative degradation products, β-apocarotenoids. Additional metabolic responses might have occurred without alteration in transcript levels of corresponding proteins. The large diversity of primary β-apocarotenoids derivatives which are expected to be formed *in planta* most likely represent intermediates, which are fueled into subsequent metabolic routes, including glycosylations and esterifications. We uncovered these processes by provoking enhanced apocarotenoid abundance through a transgenic approach; however, these metabolic routes might represent the default detoxification mode in WT tissues even with low carotenoid levels and accordingly reduced apocarotenoid formation, such as Arabidopsis roots. The interesting question of whether crops with specialized tissues accumulating high amounts of carotenoids have optimized these processes can now be approached to further improve our understanding of the interrelation between carotenoid biosynthesis and degradation.

Materials and methods

Root growth and treatments

For root generation, Arabidopsis (*A. thaliana*) plants were grown hydroponically according to (Hétu et al., 2005) for 2 weeks in liquid medium. For lipid hydroperoxide induction, H_2O_2 and *tert*-butyl hydroperoxide were added to the medium with 1 M and 100 mM final concentration, respectively, and flasks were continued shaking until roots were harvested after 4 h.

RNA Seq and RT-qPCR analysis

RNA was isolated from roots of Arabidopsis wild-type ecotype Wassilewskija and two lines overexpressing *At*PSY (line #12 and line #22, Maass et al., 2009). RNA-Seq libraries were prepared and sequenced with 100 nt single-reads on an Illumina HiSeq4000 platform. Total reads varied between 43 and 125 million reads per sample; sequencing quality was very high with about 93% of base scores above 30 in average. Quality checks of the reads were performed using fastQC (Andrews, 2010). Raw reads were trimmed using Trimmomatic (v0.32, Bolger et al., 2014). Trimmed reads were aligned using gsnap (v2016-11-07, Wu and Nacu, 2010) against the *Arabidopsis thaliana* reference genome (Ensembl TAIR10). The TAIR10 annotation version was used (Lamesch et al., 2012). Only the best alignment for each read was kept for gene expression quantification, which was performed with HTSeq-count (v.6.0.0, Anders et al., 2015). Genes with a "count per million" value greater than 0.3 (cpm $\geqslant$0.3) in at least three libraries were considered as expressed. The count normalization (calcNormFactors with "RLE" method) and detection of DEGs (GLM method) were performed using R (v.3.3.2) and the edgeR package (Robinson et al., 2010). Genes were considered differentially expressed when the FDR was below 0.05 (FDR $<$0.05).

RNA extraction and RT-qPCR analysis was performed as described in Maass et al. (2009). Primer and probe sequence information is given in Supplemental DataSet S5.

Lipid peroxide analyses

Lipid hydroperoxides were determined and quantified by the FOX2 assay, which uses the absorption of a ferric ions/xylenol orange complex formed through oxidation of ferrous ions by lipid hydroxyperoxides (DeLong et al., 2002). Two hundred milligram of roots were ground in liquid nitrogen and extracted with 1 mL of 80% (v/v) ethanol containing 0.01% (w/v) butylated hydroxytoluene. For lipid hydroperoxide analysis, extracts were diluted to a volume of 100 µL by adding methanol. Lipid hydroperoxides of one sample set were reduced by adding 100 µL of 100 mM triphenylphosphine (+TPP), while 100 µL methanol was added to the nontreated duplicate (−TPP). After 30 min incubation at RT, 1.8 mL of FOX reagent was added, the absorption at 560 nm was measured after 10 min incubation, and the difference between −TPP and +TPP was determined and converted into H_2O_2 concentrations yielding equivalent absorption.

For detailed hydroxyl fatty acid analyses, lipids were extracted from 250 mg frozen roots from hydroponically grown plants using 500-ng 15-hydroxy-eicosadienoic acid as an internal standard according to (Zoeller et al., 2012). Total hydrolysis was performed with the extracts according to (Triantaphylidès et al., 2008) thus allowing to quantify free and esterified hydroxyl fatty acids.

Carotenoids and apocarotenoid analysis

Lipophilic compounds of lyophilized roots were extracted as described in (Álvarez et al., 2016). Carotenoid and apocarotenoid quantification from plant tissues were performed as described in (Schaub et al., 2018).

ABA and PA analysis

PA and ABA were quantified according to Turečková et al. (2009) and Da Silva et al. (2012). Lyophilized, ground Arabidopsis roots (50–100 mg) were spiked with 50 ng each

of d_3-PA (Plant Biotechnology Institute, Saskatoon, Canada) and d_6-ABA (IconIsotopes, Dexter, USA) and extracted with 1 mL of methanol: water: acetic acid (10: 89: 1, v/v/v) for 1 h at 4°C. After centrifugation (10 min, 4000*g*, 4°C) the supernatant was transferred into a new tube, and the pellet re-extracted for 30 min as above. Both extracts were combined and loaded onto 1 mL Oasis® HLB cartridges (30 mg, Waters, Milford, USA), which were conditioned with 2-mL methanol and equilibrated with 2 mL of methanol: water: acetic acid (10: 89: 1, v/v/v). The cartridge was washed with 1-mL methanol: water: acetic acid (10: 89: 1; v/v/v) and eluted with 2-mL methanol: water: acetic acid (80:19:1; v/v/v). The eluate was vacuum-dried and resuspended with 40 µL of methanol: water (30:70, v/v) containing 0.1% (v/v) formic acid. Two microliters were used for LC–MS analysis (UltiMate 3000 UPLC, Q-Exactive; Thermo Scientific). Separation was achieved with a Hypersil Gold C_{18} UPLC-column (150 × 2.1 mm^2 i.d., 1.9 µm, Thermo Scientific) with the solvent system A, 0.1% formic acid in water and B, 0.1% formic acid in methanol. The gradient was developed from 30% to 50% B in 7.5 min. The column was washed with 100% B for 5 min, and initial conditions were restored within 4 min with a constant flow rate of 0.2 mL/min. Samples were analyzed in negative electrospray ionization mode. Nitrogen was used as sheath and auxiliary gas, set to 40 and 15 arbitrary units, respectively. Probe heater temperature was set to 300°C and ion spray voltage was −3 kV. MS^2-spectra for verification were generated by parallel reaction monitoring using a normalized collision energy of 40 arbitrary units. Standard curves for quantification were obtained with unlabeled PA (Plant Biotechnology Institute, Saskatoon, Canada) from 0.004 to 5 ng on-column containing 2.5 ng of d_3-PA. For ABA (Sigma-Aldrich, Germany), the range was 0.04–1.25 ng with 2.5 ng of d_6-ABA.

Enzyme assays

In general, recombinant enzymes were expressed and purified as described (AER, Mano et al., 2000; AKR4C8 and AKR4C9, Simpson et al., 2009; ChlADR, Yamauchi et al., 2011; ALDH3H1 and ALDH3I1, Stiti et al., 2011b), incubated with substrates, extracted and analyzed by GC–MS for volatile substrates (β-ionone, β-cyclocitral) and by HPLC-DAD or LC–MS for all other substrates. For detailed enzyme assay methods, see Supplemental Methods.

Accession numbers

Raw RNA-Seq data from this article can be found in the European Nucleotide Archive (http://www.ebi.ac.uk/ena/) under accession number ERP122176. AGI locus identifiers for apocarotenoid-metabolizing enzymes are as follows: AKR4C8 (At2g37760), AKR4C9 (At2g37770), ChlADR (At3g04000), AER (At5g16970), ALDH3H1 (At1g44170), ALDH3I1 (At4g34240).

Supplemental data

The following materials are available in the online version of this article.

Supplemental Figure S1 Expression levels of selected genes in carotenoid accumulating roots.

Supplemental Figure S2 β-Apocarotenoids converted by AER.

Supplemental Figure S3 GC-MS and LC-MS analysis of AER in vitro activity on β-apocarotenoids.

Supplemental Figure S4 β-Apocarotenoids converted by AKR4C8 and AKR4C9.

Supplemental Figure S5 HPLC analysis of AKR4C8 and AKR4C9 in vitro activity on β-apocarotenoids.

Supplemental Figure S6 β-Apocarotenoids converted by ChlADR.

Supplemental Figure S7 HPLC analysis of ChlADR in vitro activity on β-apocarotenoids.

Supplemental Figure S8 LC–MS analysis of conversion of apocarotenoids by AtAKR4C8, AtAKR4C9, and AtADR.

Supplemental Figure S9 β-Apocarotenoids converted by ALDH3H1 and ALDH3I1.

Supplemental Figure S10 HPLC analysis of ALDH3H1 and ALDH3I1 in vitro activity on β-apocarotenoids.

Supplemental Figure S11 LC–MS analysis of conversion of apocarotenoids by ALDH3I1and ALDH3H1.

Supplemental Figure S12 Mass spectrometric identification of apocarotenoids.

Supplemental Table S1 In vitro conversion of various oxidative β-carotene degradation products.

Supplemental Dataset S1 Analysis of carotenoid and MEP pathway specific genes.

Supplemental Dataset S2 Overrepresentation analysis.

Supplemental Dataset S3 Intersection *At12*/*At22* with β-cyclocitral treatment.

Supplemental Dataset S4 Up and downregulated genes in carotenoid accumulating Arabidopsis roots, lines *At12* and *At22*.

Supplemental Dataset S5 Primer and probes.

Supplemental Methods Detailed information on in vitro enzyme assays.

Acknowledgments

We are indebted to Klaus Palme (University of Freiburg) for providing strong support to realize this project. We thank Carmen Schubert (University of Freiburg) for her skillful technical assistance and Glendis Shiko (University of Freiburg) for his assistance. We acknowledge the ABRC (Arabidopsis Biological Resource Center) and S.P. Dinesh-Kumar and M. Snyder for providing Arabidopsis GGPS cDNA clones. We thank GenomEast platform (IGBMC, France) for the RNA sequencing. We thank Amandine Velt for her help with data submission to the European Nucleotide Archive (ENA).

Funding

This work was supported by the HarvestPlus research consortium (grant 2014H6320.FRE) to R.W., by the Deutsche Forschungsgemeinschaft (grant WE4731/3) to J.K. and by a grant from the University of Strasbourg's Institute for Advanced Studies to D.T., P.H., and P.B.

Conflict of interest statement. None declared.

References

Ahrazem O, Gómez-Gómez L, Rodrigo M, Avalos J, Limón M (2016) Carotenoid cleavage oxygenases from microbes and photosynthetic organisms: features and functions. Int J Mol Sci **17**: 1781

Ahrazem O, Rubio-Moraga A, Berman J, Capell T, Christou P, Zhu C, Gómez-Gómez L (2015a) The carotenoid cleavage dioxygenase CCD2 catalysing the synthesis of crocetin in spring crocuses and saffron is a plastidial enzyme. New Phytol, **209**: 650–663

Ahrazem O, Rubio-Moraga A, Nebauer SG, Molina RV, Gómez-Gómez L (2015b) Saffron: its phytochemistry, developmental processes, and biotechnological prospects. J Agric Food Chem **63**: 8751–8764

Alder A, Jamil M, Marzorati M, Bruno M, Vermathen M, Bigler P, Ghisla S, Bouwmeester H, Beyer P, Al-Babili S (2012) The path from b-carotene to carlactone, a strigolactone-like plant hormone. Science **335**: 1348–1351

Álvarez D, Voß B, Maass D, Wüst F, Schaub P, Beyer P, Welsch R (2016) Carotenogenesis is regulated by 5′UTR-mediated translation of phytoene synthase splice variants. Plant Physiol **172**: 2314–2326

Amara I, Zaidi I, Masmoudi K, Ludevid MD, Pagès M, Goday A, Brini F (2014) Insights into late embryogenesis abundant (LEA) proteins in plants: from structure to the functions. Am J Plant Sci **5**: 3440–3455

Anders S, Pyl PT, Huber W (2015) HTSeq–a Python framework to work with high-throughput sequencing data. Bioinformatics **31**: 166–169

Andrews S (2010) FastQC: a quality control tool for high throughput sequence data. https://www.bioinformatics.babraham.ac.uk/projects/fastqc (June 24, 2020)

Arango J, Jourdan M, Geoffriau E, Beyer P, Welsch R (2014) Carotene hydroxylase activity determines the levels of both α-carotene and total carotenoids in orange carrots. Plant Cell **26**: 2223–2233

Baerson SR, Sánchez-Moreiras A, Pedrol-Bonjoch N, Schulz M, Kagan IA, Agarwal AK, Reigosa MJ, Duke SO (2005) Detoxification and transcriptome response in Arabidopsis seedlings exposed to the allelochemical benzoxazolin-2(3H)-one. J Biol Chem **280**: 21867–21881

Bai L, Kim E-H, DellaPenna D, Brutnell TP (2009) Novel lycopene epsilon cyclase activities in maize revealed through perturbation of carotenoid biosynthesis. Plant J **59**: 588–599

Baranski R, Cazzonelli CI (2016) Carotenoid Biosynthesis and Regulation in Plants. John Wiley & Sons, Ltd, Chichester, UK, pp. 159–189

Beck G, Coman D, Herren E, Ruiz-Sola MA, Rodríguez-Concepción M, Gruissem W, Vranová E (2013) Characterization of the GGPP synthase gene family in Arabidopsis thaliana. Plant Mol Biol **82**: 393–416

Beisel KG, Jahnke S, Hofmann D, Koppchen S, Schurr U, Matsubara S (2010) Continuous turnover of carotenes and chlorophyll a in mature leaves of Arabidopsis thaliana revealed by 14CO2 pulse-chase labeling. Plant Physiol **152**: 2188–2199

Beisel KG, Schurr U, Matsubara S (2011) Altered turnover of β-carotene and Chl a in Arabidopsis leaves treated with lincomycin or norflurazon. Plant Cell Physiol **52**: 1193–1203

Ben-Shaul Y, Naftali Y (1969) The development and ultrastructure of lycopene bodies in chromoplasts of Lycopersicum esculentum. Protoplasma **67**: 333–344

Beyer P, Al-Babili S, Ye X, Lucca P, Schaub P, Welsch R, Potrykus I (2002) Golden Rice: introducing the beta-carotene biosynthesis pathway into rice endosperm by genetic engineering to defeat vitamin A deficiency. J Nutr **132**: 506S–510S

Bolger AM, Lohse M, Usadel B (2014) Trimmomatic: a flexible trimmer for Illumina sequence data. Bioinformatics **30**: 2114–2120

Britton G (1995) Structure and properties of carotenoids in relation to function. FASEB J **9**: 1551–1558

Bruno M, Beyer P, Al-Babili S (2015) The potato carotenoid cleavage dioxygenase 4 catalyzes a single cleavage of β-ionone ring-containing carotenes and non-epoxidated xanthophylls. Arch Biochem Biophys **572**: 126–133

Burla B, Pfrunder S, Nagy R, Francisco RM, Lee Y, Martinoia E (2013) Vacuolar transport of abscisic acid glucosyl ester is mediated by ATP-binding cassette and proton-antiport mechanisms in Arabidopsis. Plant Physiol **163**: 1446–1458

Burton GW, Daroszewski J, Mogg TJ, Nikiforov GB, Nickerson JG (2016) Discovery and characterization of carotenoid-oxygen copolymers in fruits and vegetables with potential health benefits. J Agric Food Chem **64**: 3767–3777

Burton GW, Daroszewski J, Nickerson JG, Johnston JB, Mogg TJ, Nikiforov GB (2014) β-Carotene autoxidation: oxygen copolymerization, non-vitamin A products, and immunological activity. Can J Chem **92**: 305–316

Camagna M, Grundmann A, Bär C, Koschmieder J, Beyer P, Welsch R (2019) Enzyme fusion removes competition for geranylgeranyl diphosphate in carotenogenesis. Plant Physiol **179**: 1013–1027

Carretero-Paulet L, Cairó A, Botella-Pavía P, Besumbes O, Campos N, Boronat A, Rodríguez-Concepción M (2006) Enhanced flux through the methylerythritol 4-phosphate pathway in Arabidopsis plants overexpressing deoxyxylulose 5-phosphate reductoisomerase. Plant Mol Biol **62**: 683–695

Cazzonelli C, Pogson BJ (2010) Source to sink: regulation of carotenoid biosynthesis in plants. Trends Plant Sci **15**: 266–274

Clícia Maria de Jesus B, da Cunha Veloso MC, de Paula Pereira PA, de Andrade JB (2011) A chemical study of β-carotene oxidation by ozone in an organic model system and the identification of the resulting products. Food Chem **126**: 927–934

Da Silva CMS, Habermann G, Marchi MRR, Zocolo GJ (2012) The role of matrix effects on the quantification of abscisic acid and its metabolites in the leaves of Bauhinia variegata L. using liquid chromatography combined with tandem mass spectrometry. Brazilian J Plant Physiol **24**: 223–232

D'Alessandro S, Havaux M (2019) Sensing β-carotene oxidation in photosystem II to master plant stress tolerance. New Phytol **223**: 1776–1783

D'Alessandro S, Ksas B, Havaux M (2018) Decoding β-cyclocitral-mediated retrograde signaling reveals the role of a detoxification response in plant tolerance to photooxidative stress. Plant Cell **30**: 2495–2511

Darley CP, Forrester AM, McQueen-Mason SJ (2001) The molecular basis of plant cell wall extension. Plant Mol Biol **47**: 179–195

DeLong JM, Prange RK, Hodges DM, Forney CF, Bishop MC, Quilliam M (2002) Using a modified ferrous oxidation-xylenol orange (FOX) assay for detection of lipid hydroperoxides in plant tissue. J Agric Food Chem **50**: 248–254

Demurtas OC, de Brito Francisco R, Martinoia E, Giuliano G (2020) Transportomics for the Characterization of Plant Apocarotenoid Transmembrane Transporters. Humana, New York, NY, pp. 89–99

Demurtas OC, Francisco R, Diretto G, Ferrante P, Frusciante S, Pietrella M, Aprea G, Borghi L, Feeney M, Frigerio L, et al. (2019) ABCC transporters mediate the vacuolar accumulation of crocins in saffron stigmas. Plant Cell **31**: 2789–2804

Demurtas OC, Frusciante S, Ferrante P, Diretto G, Azad NH, Pietrella M, Aprea G, Taddei AR, Romano E, Mi J, et al. (2018) Candidate enzymes for saffron crocin biosynthesis are localized in multiple cellular compartments. Plant Physiol **177**: 990–1006

Dickinson AJ, Lehner K, Mi J, Jia K-P, Mijar M, Dinneny J, Al-Babili S, Benfey PN (2019) β-Cyclocitral is a conserved root growth regulator. Proc Natl Acad Sci USA **116**: 10563–10567

Diretto G, Ahrazem O, Rubio-Moraga Á, Fiore A, Sevi F, Argandoña J, Gómez-Gómez L (2019) UGT709G1: a novel uridine diphosphate glycosyltransferase involved in the biosynthesis of picrocrocin, the precursor of safranal in saffron (Crocus sativus) . New Phytol **224**: 725–740

Diretto G, Welsch R, Tavazza R, Mourgues F, Pizzichini D, Beyer P, Giuliano G (2007) Silencing of beta-carotene hydroxylase increases total carotenoid and beta-carotene levels in potato tubers. BMC Plant Biol **7**: 11

Dong T, Xu Z-Y, Park Y, Kim DH, Lee Y, Hwang I (2014) Abscisic acid uridine diphosphate glucosyltransferases play a crucial role in abscisic acid homeostasis in Arabidopsis. Plant Physiol **165**: 277–289

Edqvist J, Blomqvist K, Nieuwland J, Salminen TA (2018) Plant lipid transfer proteins: are we finally closing in on the roles of these enigmatic proteins? J Lipid Res **59**: 1374–1382

Farmer EE, Davoine C (2007) Reactive electrophile species. Curr Opin Plant Biol **10**: 380–386

Farmer EE, Mueller MJ (2013) ROS-mediated lipid peroxidation and RES-activated signaling. Annu Rev Plant Biol **64**: 429–450

Farré G, Sanahuja G, Naqvi S, Bai C, Capell T, Zhu C, Christou P (2010) Travel advice on the road to carotenoids in plants. Plant Sci **179**: 28–48

Felemban A, Braguy J, Zurbriggen MD, Al-Babili S (2019) Apocarotenoids involved in plant development and stress response. Front Plant Sci **10**: 1168

Frusciante S, Diretto G, Bruno M, Ferrante P, Pietrella M, Prado-Cabrero A, Rubio-Moraga A, Beyer P, Gomez-Gomez L, Al-Babili S, et al. (2014) Novel carotenoid cleavage dioxygenase catalyzes the first dedicated step in saffron crocin biosynthesis. Proc Natl Acad Sci USA **111**: 12246–12251

Gonzalez-Jorge S, Ha S-H, Magallanes-Lundback M, Gilliland LU, Zhou A, Lipka AE, Nguyen Y-N, Angelovici R, Lin H, Cepela J, et al. (2013) *CAROTENOID CLEAVAGE DIOXYGENASE4* is a negative regulator of β-carotene content in Arabidopsis seeds. Plant Cell **25**: 4812–4826

Grimsrud PA, Xie H, Griffin TJ, Bernlohr DA (2008) Oxidative stress and covalent modification of protein with bioactive aldehydes. The Journal of biological chemistry **283**: 21837–41

Harvey PJ, Campanella BF, Castro PML, Harms H, Lichtfouse E, Schäffner AR, Smrcek S, Werck-Reichhart D (2002) Phytoremediation of polyaromatic hydrocarbons, anilines and phenols. Environ Sci Pollut Res Int **9**: 29–47

Havaux M (2013) Carotenoid oxidation products as stress signals in plants. Plant J **79**: 597–606

Hétu M-F, Tremblay LJ, Lefebvre DD (2005) High root biomass production in anchored Arabidopsis plants grown in axenic sucrose supplemented liquid culture. Biotechniques **39**: 345–349

Hou X, Rivers J, León P, McQuinn RP, Pogson BJ (2016) Synthesis and function of apocarotenoid signals in plants. Trends Plant Sci **21**: 792–803

Ilg A, Beyer P, Al-Babili S (2009) Characterization of the rice carotenoid cleavage dioxygenase 1 reveals a novel route for geranial biosynthesis. FEBS J **276**: 736–747

Jeffery J, Holzenburg A, King S (2012) Physical barriers to carotenoid bioaccessibility. Ultrastructure survey of chromoplast and cell wall morphology in nine carotenoid-containing fruits and vegetables. J Sci Food Agric **92**: 2594–2602

Kachanovsky DE, Filler S, Isaacson T, Hirschberg J (2012) Epistasis in tomato color mutations involves regulation of phytoene synthase 1 expression by cis-carotenoids. Proc Natl Acad Sci USA **109**: 19021–19026

Kang J, Park J, Choi H, Burla B, Kretzschmar T, Lee Y, Martinoia E (2011) Plant ABC transporters. Arab B **9**: e0153

Kim J, Smith JJ, Tian L, DellaPenna D (2009) The evolution and function of carotenoid hydroxylases in Arabidopsis. Plant Cell Physiol **50**: 463–479

Koschmieder J, Welsch R (2020) Quantification of carotenoid pathway flux in green and nongreen systems. Methods Mol Biol 2083: 279–291

Lamesch P, Berardini TZ, Li D, Swarbreck D, Wilks C, Sasidharan R, Muller R, Dreher K, Alexander DL, Garcia-Hernandez M, et al. (2012) The Arabidopsis Information Resource (TAIR): improved gene annotation and new tools. Nucleic Acids Res **40**: D1202–D1210

Lätari K, Wüst F, Hübner M, Schaub P, Beisel, Kim G, Matsubara S, Beyer P, Welsch R (2015) Tissue-specific apocarotenoid glycosylation contributes to carotenoid homeostasis in Arabidopsis leaves. Plant Physiol **168**: 1550–1562

von Lintig J, Welsch R, Bonk M, Giuliano G, Batschauer A, Kleinig H (1997) Light-dependent regulation of carotenoid biosynthesis occurs at the level of phytoene synthase expression and is mediated by phytochrome in Sinapis alba and Arabidopsis thaliana seedlings. Plant J **12**: 625–634

Lois LM, Rodríguez-Concepción M, Gallego F, Campos N, Boronat A (2000) Carotenoid biosynthesis during tomato fruit development: regulatory role of 1-deoxy-D-xylulose 5-phosphate synthase. Plant J **22**: 503–513

Maass D, Arango J, Wüst F, Beyer P, Welsch R (2009) Carotenoid crystal formation in Arabidopsis and carrot roots caused by increased phytoene synthase protein levels. PLoS One **4**: e6373

Mano J (2012) Reactive carbonyl species: their production from lipid peroxides, action in environmental stress, and the detoxification mechanism. Plant Physiol Biochem **59**: 90–97

Mano J, Torii Y, Hayashi S, Takimoto K, Matsui K, Nakamura K, Inzé D, Babiychuk E, Kushnir S, Asada K (2002) The NADPH:quinone oxidoreductase P1-zeta-crystallin in Arabidopsis catalyzes the alpha,beta-hydrogenation of 2-alkenals: detoxication of the lipid peroxide-derived reactive aldehydes. Plant Cell Physiol **43**: 1445–1455

Mano J, Babiychuk E, Belles-Boix E, Hiratake J, Kimura A, Inzé D, Kushnir S, Asada K (2000) A novel NADPH:diamide oxidoreductase activity in Arabidopsis thaliana P1 ζ-crystallin. Eur J Biochem **267**: 3661–3671

Mano J, Belles-Boix E, Babiychuk E, Inzé D, Torii Y, Hiraoka E, Takimoto K, Slooten L, Asada K, Kushnir S (2005) Protection against photooxidative injury of tobacco leaves by 2-alkenal reductase. Detoxication of lipid peroxide-derived reactive carbonyls. Plant Physiol **139**: 1773–1783

Mano J, Biswas MS, Sugimoto K (2019a) Reactive carbonyl species: a missing link in ROS signaling. Plants **8**: 391

Mano J, Kanameda S, Kuramitsu R, Matsuura N, Yamauchi Y (2019b) Detoxification of reactive carbonyl species by glutathione transferase tau isozymes. Front Plant Sci **10**: 487

McNulty HP, Byun J, Lockwood SF, Jacob RF, Mason RP (2007) Differential effects of carotenoids on lipid peroxidation due to membrane interactions: X-ray diffraction analysis. Biochim Biophys Acta – Biomembr **1768**: 167–174

Mi H, Muruganujan A, Casagrande JT, Thomas PD (2013) Large-scale gene function analysis with the PANTHER classification system. Nat Protoc **8**: 1551–1566

Mosblech A, Feussner I, Heilmann I (2009) Oxylipins: structurally diverse metabolites from fatty acid oxidation. Plant Physiol Biochem **47**: 511–517

Mueller S, Hilbert B, Dueckershoff K, Roitsch T, Krischke M, Mueller MJ, Berger S (2008) General detoxification and stress responses are mediated by oxidized lipids through TGA transcription factors in Arabidopsis. Plant Cell **20**: 768–785

Niyogi KK, Grossman AR, Björkman O (1998) Arabidopsis mutants define a central role for the xanthophyll cycle in the regulation of photosynthetic energy conversion. Plant Cell **10**: 1121–1134

Nogueira M, Mora L, Enfissi EMA, Bramley PM, Fraser PD (2013) Subchromoplast sequestration of carotenoids affects regulatory mechanisms in tomato lines expressing different carotenoid gene combinations. Plant Cell **25**: 4560–4579

Paolillo DJ, Garvin DF, Parthasarathy MV (2004) The chromoplasts of Or mutants of cauliflower (Brassica oleracea L. var. botrytis). Protoplasma **224**: 245–253

Park AR, Cho SK, Yun UJ, Jin MY, Lee SH, Sachetto-Martins G, Park OK (2001) Interaction of the Arabidopsis receptor protein kinase Wak1 with a glycine-rich protein, AtGRP-3. J Biol Chem **276**: 26688–26693

Ramel F, Birtic S, Cuiné S, Triantaphylidès C, Ravanat J-L, Havaux M (2012a) Chemical quenching of singlet oxygen by carotenoids in plants. Plant Physiol **158**: 1267–1278

Ramel F, Birtic S, Ginies C, Soubigou-Taconnat L, Triantaphylidès C, Havaux M (2012b) Carotenoid oxidation products are stress signals that mediate gene responses to singlet oxygen in plants. Proc Natl Acad Sci USA **109**: 5535–5540

Ramel F, Sulmon C, Serra A-A, Gouesbet G, Couee I (2012c) Xenobiotic sensing and signalling in higher plants. J Exp Bot **63**: 3999–4014

Robinson MD, McCarthy DJ, Smyth GK (2010) edgeR: a Bioconductor package for differential expression analysis of digital gene expression data. Bioinformatics **26**: 139–140

Rodríguez-Concepción M, Ahumada I, Diez-Juez E, Sauret-Güeto S, Lois LM, Gallego F, Carretero-Paulet L, Campos N, Boronat A (2001) 1-Deoxy-D-xylulose 5-phosphate reductoisomerase and plastid isoprenoid biosynthesis during tomato fruit ripening. Plant J **27**: 213–222

Rubio A, Rambla JL, Santaella M, Gómez MD, Orzaez D, Granell A, Gómez-Gómez L (2008) Cytosolic and plastoglobule-targeted carotenoid dioxygenases from Crocus sativus are both involved in beta-ionone release. J Biol Chem **283**: 24816–24825

Ruiz-Sola MÁ, Barja MV, Manzano D, Llorente B, Schipper B, Beekwilder J, Rodriguez-Concepcion M (2016a) A single gene encodes two differentially targeted geranylgeranyl diphosphate synthase isoforms. Plant Physiol **172**: 1393–1402

Ruiz-Sola MÁ, Coman D, Beck G, Barja MV, Colinas M, Graf A, Welsch R, Rütimann P, Bühlmann P, Bigler L, et al. (2016b) Arabidopsis GERANYLGERANYL DIPHOSPHATE SYNTHASE 11 is a hub isozyme required for the production of most photosynthesis-related isoprenoids. New Phytol **209**: 252–264

Saito R, Shimakawa G, Nishi A, Iwamoto T, Sakamoto K, Yamamoto H, Amako K, Makino A, Miyake C (2013) Functional analysis of the AKR4C subfamily of arabidopsis thaliana: model structures, substrate specificity, acrolein toxicity, and responses to light and [CO_2]. Biosci Biotechnol Biochem **77**: 2038–2045

Salminen TA, Blomqvist K, Edqvist J (2016) Lipid transfer proteins: classification, nomenclature, structure, and function. Planta **244**: 971–997

Sandermann H (1992) Plant metabolism of xenobiotics. Trends Biochem Sci **17**: 82–84

Sattler SE, Mène-Saffrané L, Farmer EE, Krischke M, Mueller MJ, DellaPenna D (2006) Nonenzymatic lipid peroxidation reprograms gene expression and activates defense markers in Arabidopsis tocopherol-deficient mutants. Plant Cell **18**: 3706–3720

Schaub P, Rodriguez-Franco M, Cazzonelli CI, Álvarez D, Wüst F, Welsch R (2018) Establishment of an Arabidopsis callus system to study the interrelations of biosynthesis, degradation and accumulation of carotenoids. PLoS One **13**: e0192158

Schaub P, Wuest F, Koschmieder J, Yu Q, Virk P, Tohme J, Beyer P (2017) Non-enzymatic β-carotene degradation in (provitamin A-biofortified) crop plants. J Agric Food Chem **65**

Schweiggert RM, Mezger D, Schimpf F, Steingass CB, Carle R (2012) Influence of chromoplast morphology on carotenoid bioaccessibility of carrot, mango, papaya, and tomato. Food Chem **135**: 2736–2742

Sengupta D, Naik D, Reddy AR (2015) Plant aldo-keto reductases (AKRs) as multi-tasking soldiers involved in diverse plant metabolic processes and stress defense: a structure-function update. J Plant Physiol **179**: 40–55

Simkin AJ, Underwood BA, Auldridge ME, Loucas HM, Shibuya K, Schmelz E, Clark DG, Klee HJ (2004) Circadian Regulation of the PhCCD1 Carotenoid Cleavage Dioxygenase Controls Emission of ß-Ionone, a Fragrance Volatile of Petunia Flowers. Plant Physiology **136**: 3504–3514

Simkin AJ, Zhu C, Kuntz M, Sandmann G (2003) Light-dark regulation of carotenoid biosynthesis in pepper (Capsicum annuum) leaves. J Plant Physiol **160**: 439–443

Simpson PJ, Tantitadapitak C, Reed AM, Mather OC, Bunce CM, White SA, Ride JP (2009) Characterization of two novel aldo–keto reductases from Arabidopsis: expression patterns, broad substrate specificity, and an open active-site structure suggest a role in toxicant metabolism following stress. J Mol Biol **392**: 465–480

Stiti N, Adewale IO, Petersen J, Bartels D, Kirch H-H (2011a) Engineering the nucleotide coenzyme specificity and sulfhydryl redox sensitivity of two stress-responsive aldehyde dehydrogenase isoenzymes of Arabidopsis thaliana. Biochem J **434**: 459–471

Stiti N, Missihoun TD, Kotchoni SO, Kirch H-H, Bartels D (2011b) Aldehyde dehydrogenases in arabidopsis thaliana: biochemical requirements, metabolic pathways, and functional analysis. Front Plant Sci **2**: 65

Stotz HU, Mueller S, Zoeller M, Mueller MJ, Berger S (2013) TGA transcription factors and jasmonate-independent COI1 signalling regulate specific plant responses to reactive oxylipins. J Exp Bot **64**: 963–975

Taleon V, Mugode L, Cabrera-Soto L, Palacios-Rojas N (2017) Carotenoid retention in biofortified maize using different post-harvest storage and packaging methods. Food Chem **232**: 60–66

Tan B-C, Joseph LM, Deng W-T, Liu L, Li Q-B, Cline K, McCarty DR (2003) Molecular characterization of the Arabidopsis 9 -cis epoxycarotenoid dioxygenase gene family. Plant J **35**: 44–56

Tenhaken R (2015) Cell wall remodeling under abiotic stress. Front Plant Sci **5**: 771

Tian L, Magallanes-Lundback M, Musetti V, DellaPenna D (2003) Functional analysis of beta- and epsilon-ring carotenoid hydroxylases in Arabidopsis. Plant Cell **15**: 1320–1332

Tomita K, Hasegawa M, Arii S, Tsuji K, Bober B, Harada K (2016) Characteristic oxidation behavior of β-cyclocitral from the cyanobacterium Microcystis. Environ Sci Pollut Res **23**: 11998–12006

Trautmann D, Beyer P, Al-Babili S (2013) The ORF slr0091 of Synechocystis sp. PCC6803 encodes a high-light induced aldehyde dehydrogenase converting apocarotenals and alkanals. FEBS J **280**: 3685–3696

Triantaphylidès C, Krischke M, Hoeberichts FA, Ksas B, Gresser G, Havaux M, Van Breusegem F, Mueller MJ (2008) Singlet oxygen is the major reactive oxygen species involved in photooxidative damage to plants. Plant Physiol **148**: 960–968

Turečková V, Novák O, Strnad M (2009) Profiling ABA metabolites in Nicotiana tabacum L. leaves by ultra-performance liquid chromatography–electrospray tandem mass spectrometry. Talanta **80**: 390–399

Walter MH, Strack D (2011) Carotenoids and their cleavage products: biosynthesis and functions. Nat Prod Rep **28**: 663–692

Wang Y, Bouwmeester HJ (2018) Structural diversity in the strigolactones. J Exp Bot **69**: 2219–2230

Weber H, Chételat A, Reymond P, Farmer EE (2004) Selective and powerful stress gene expression in Arabidopsis in response to malondialdehyde. Plant J **37**: 877–888

Weisman D, Alkio M, Colón-Carmona A, Meudec A, Poupart N, Dussauze J, Deslandes E, Oros D, Ross J, Spies R, et al. (2010) Transcriptional responses to polycyclic aromatic hydrocarbon-induced stress in Arabidopsis thaliana reveal the involvement of hormone and defense signaling pathways. BMC Plant Biol **10**: 59

Welsch R, Wüst F, Bär C, Al-Babili S, Beyer P (2008) A third phytoene synthase is devoted to abiotic stress-induced abscisic acid

formation in rice and defines functional diversification of phytoene synthase genes. Plant Physiol **147**: 367–80

Welsch R, Zhou X, Yuan H, Álvarez D, Sun T, Schlossarek D, Yang Y, Shen G, Zhang H, Rodriguez-Concepcion M, et al. (2017) Clp protease and OR directly control the proteostasis of phytoene synthase, the crucial enzyme for carotenoid biosynthesis in Arabidopsis. Mol Plant **11**: 149–162

Winterhalter P, Rouseff RL (2001) Carotenoid-Derived Aroma Compounds (Acs Symposium Series). American Chemical Society Publication, Washington.

Wu TD, Nacu S (2010) Fast and SNP-tolerant detection of complex variants and splicing in short reads. Bioinformatics **26**: 873–881

Wu Z, Robinson DS, Hughes RK, Casey R, Hardy D, West SI (1999) Co-oxidation of beta-carotene catalyzed by soybean and recombinant pea lipoxygenases. J Agric Food Chem **47**: 4899–4906

Wurtzel ET (2019) Changing form and function through carotenoids and synthetic biology. Plant Physiol **179**: 830–843

Yamauchi Y, Hasegawa A, Mizutani M, Sugimoto Y (2012) Chloroplastic NADPH-dependent alkenal/one oxidoreductase contributes to the detoxification of reactive carbonyls produced under oxidative stress. FEBS Lett **586**: 1208–1213

Yamauchi Y, Hasegawa A, Taninaka A, Mizutani M, Sugimoto Y (2011) NADPH-dependent reductases involved in the detoxification of reactive carbonyls in plants. J Biol Chem **286**: 6999–7009

Yamauchi Y, Kunishima M, Mizutani M, Sugimoto Y (2015) Reactive short-chain leaf volatiles act as powerful inducers of abiotic stress-related gene expression. Sci Rep **5**: 8030

Yanishlieva NV., Aitzetmüller K, Raneva V (1998) β-Carotene and lipid oxidation. Fett/Lipid **100**: 444–462

Young TE, Gallie DR (2000) Programmed cell death during endosperm development. Plant Mol Biol **44**: 283–301

Yuan H, Zhang J, Nageswaran D, Li L (2015) Carotenoid metabolism and regulation in horticultural crops. Hortic Res **2**: 15036

Zoeller M, Stingl N, Krischke M, Fekete A, Waller F, Berger S, Mueller MJ (2012) Lipid profiling of the Arabidopsis hypersensitive response reveals specific lipid peroxidation and fragmentation processes: biogenesis of pimelic and azelaic acid. Plant Physiol **160**: 365–378